JPn Neuroscience
The Journal of Physiology
J Physiol 591.7 (2013) pp 1671–1689

Nanomolar ouabain augments Ca^{2+} signalling in rat hippocampal neurones and glia

Hong Song[1], Scott M. Thompson[1,2] and Mordecai P. Blaustein[1,3]

Departments of [1]Physiology, [2]Psychiatry and [3]Medicine, University of Maryland School of Medicine, Baltimore, MD, USA

Key points

- Co-cultured rat hippocampal neurons and astrocytes express high-ouabain-affinity Na^+ pumps with, respectively, $\alpha3$ and $\alpha2$ catalytic subunits.
- Low-dose L-glutamate (Glu) and carbachol (CCh) evoked Ca^{2+} transients in neurons; Glu also evoked small, delayed transients in some astrocytes. Low-dose ATP evoked Ca^{2+} transients only in astrocytes.
- Studies with NMDA receptors and metabotropic glutamate receptor (mGluR) blockers revealed that the neuronal Glu-evoked transients were mediated primarily by mGluR5 metabotropic receptors.
- Pre-incubation with 1–10 nM ouabain ($EC_{50} < 1$ nM) augmented neuronal Glu- and CCh-evoked Ca^{2+} transients; this augmentation was mediated by $\alpha3$ Na^+ pumps and Na^+–Ca^{2+} exchangers.
- Ouabain pre-incubation also augmented ATP-evoked astrocyte Ca^{2+} transients mediated by $\alpha2$ Na^+ pumps.
- Nanomolar ouabain and impaired $\alpha3$ and $\alpha2$ Na^+ pump activity influence Ca^{2+} signalling and may thus modulate synaptic transmission in the brain. This could explain the physiological manifestations of $\alpha3$ and $\alpha2$ pump mutations and certain mood disorders linked to altered Na^+ pump function.

Abstract Linkage of certain neurological diseases to Na^+ pump mutations and some mood disorders to altered Na^+ pump function has renewed interest in brain Na^+ pumps. We tested nanomolar ouabain on Ca^{2+} signalling (fura-2) in rat hippocampal neurone–astrocyte co-cultures. The neurones and astrocytes express Na^+ pumps with a high-ouabain-affinity catalytic subunit ($\alpha3$ and $\alpha2$, respectively); both also express pumps with a ouabain-resistant $\alpha1$ subunit. Neurones and astrocytes were identified by immunocytochemistry and by stimulation; 3–4 μM L-glutamate (Glu) and 3 μM carbachol (CCh) evoked rapid Ca^{2+} transients only in neurones, and small, delayed transients in some astrocytes, whereas 0.5–1 μM ATP evoked Ca^{2+} transients only in astrocytes. Both cell types responded to 5–10 μM Glu or ATP. The signals evoked by 3–4 μM Glu in neurones were markedly inhibited by 3–10 μM MPEP (blocks metabotropic glutamate receptor mGluR5) and 10 μM LY341495 (non-selective mGluR blocker), but not by 80 μM AP5 (NMDA receptor blocker) or by selective block of mGluR1 or mGluR2. Pre-incubation (0.5–10 min) with 1–10 nM ouabain ($EC_{50} < 1$ nM) augmented Glu- and CCh-evoked signals in neurones. This augmentation was abolished by a blocker of the Na^+–Ca^{2+} exchanger, SEA0400 (300 nM). Ouabain (3 nM) pre-incubation also augmented 10 μM cyclopiazonic acid plus 10 mM caffeine-evoked release of Ca^{2+} from the neuronal endoplasmic reticulum (ER). The implication is that nanomolar ouabain inhibits $\alpha3$ Na^+ pumps, increases (local) intracellular Na^+, and promotes Na^+–Ca^{2+} exchanger-mediated Ca^{2+} gain and increased storage in the adjacent ER.

DOI: 10.1113/jphysiol.2012.248336

Ouabain (3 nM) also increased ER Ca^{2+} release and enhanced 0.5 μM ATP-evoked transients in astrocytes; these effects were mediated by $\alpha2$ Na^+ pumps. Thus, nanomolar ouabain may strongly influence synaptic transmission in the brain as a result of its actions on the high-ouabain-affinity Na^+ pumps in both neurones and astrocytes. The significance of these effects is heightened by the evidence that ouabain is endogenous in mammals.

(Received 12 November 2012; accepted after revision 2 January 2013; first published online 7 January 2013)
Corresponding author M. P. Blaustein: Department of Physiology, University of Maryland School of Medicine, 655 West Baltimore Street, Baltimore, MD 21201, USA. Email: mblaustein@som.umaryland.edu

Abbreviations $\alpha1$ (or $\alpha2$ or $\alpha3$) Na^+ pumps, Na^+ pumps with an $\alpha1$ (or $\alpha2$ or $\alpha3$) catalytic subunit; CAF, caffeine; CCh, carbachol; CPA, cyclopiazonic acid; CTS, cardiotonic steroids; DHO, dihydro-ouabain; ER, endoplasmic reticulum; GFAP, glial fibrillary acidic protein; Glu, L-glutamate; 5-HT, serotonin; mGluR, metabotropic glutamate receptor; NCX, Na^+–Ca^{2+} exchange(r); NF-H, neurofilament-H; NMDAR, *N*-methyl-D-aspartate receptor; PM, plasma membrane; PSS, physiological salt solution.

Introduction

Sodium pumps (Na^+,K^+-ATPase) maintain the Na^+ and K^+ electrochemical gradients in virtually all mammalian cells, including neurones and glia (Blanco & Mercer, 1998). Recent pathophysiological discoveries have renewed interest in the specific roles of neuronal Na^+ pumps and their high-ouabain-affinity binding sites. First was the identification of two human neurological diseases, familial hemiplegic migraine type 2 and rapid-onset dystonia with parkinsonism, that result from loss-of-function mutations in, respectively, the $\alpha2$ and $\alpha3$ isoforms of the Na^+ pump catalytic (α) subunit (De Fusco *et al.* 2003; de Carvalho Aguiar *et al.* 2004; Brashear *et al.* 2007; de Vries *et al.* 2007). Second, a number of reports have linked altered Na^+ pump function to depressive and bipolar behaviour disorders (Coppen *et al.* 1966; Naylor *et al.* 1970; Naylor & Smith, 1981; Looney & el-Mallakh, 1997; Goldstein *et al.* 2006; Kirshenbaum *et al.* 2011).

Sodium pumps are $\alpha\beta$ dimers. The α subunit contains the cation transport machinery and the ouabain binding site (Blanco & Mercer, 1998; Lingrel, 2010). Three α isoforms, $\alpha1$–$\alpha3$, are expressed in the brain. In rodents, only $\alpha2$ and $\alpha3$ have high ouabain affinity (O'Brien *et al.* 1994), and even in humans, the $\alpha1$ isoform has ∼20- to 50-fold lower affinity for ouabain than $\alpha2$ or $\alpha3$ (Linde *et al.* 2012).

The $\alpha1$ Na^+ pumps are expressed in all cells; they are usually the most prevalent (e.g. ∼80% of all Na^+ pumps in astrocytes), and they maintain the plasma membrane (PM) Na^+ and K^+ gradients (Golovina *et al.* 2003). Most mature neurones also express $\alpha3$, while $\alpha2$ is expressed in glia, blood vessels and some neurones, especially in the neonate (McGrail *et al.* 1991; Brines & Robbins, 1993; Moseley *et al.* 2003; Song *et al.* 2006). In glia and in neurones, respectively, $\alpha2$ and $\alpha3$ Na^+ pumps co-localize with Na^+–Ca^{2+} exchangers (NCX) in PM microdomains at PM–endoplasmic reticulum (ER) junctions (Juhaszova & Blaustein, 1997*a*,*b*). This juxtaposition and proximity to the ER contributes to the roles of $\alpha2$ and $\alpha3$ Na^+ pumps in Ca^{2+} signalling.

In rodents, $\alpha2$ and $\alpha3$ Na^+ pumps, and their high-ouabain-affinity binding sites, play important roles in neuronal function and behaviour. Mice with a null mutation in one $\alpha2$ or $\alpha3$, but not $\alpha1$, allele exhibit behavioural and learning deficits, but apparently do not mimic the human familial hemiplegic migraine or rapid-onset dystonia with parkinsonism phenotypes, respectively (Ikeda *et al.* 2003; Lingrel *et al.* 2007; Moseley *et al.* 2007). Heterozygous $\alpha2$ ($\alpha2^{+/-}$) mice have enhanced anxiety and fear, and impaired long-term memory (Ikeda *et al.* 2003; Lingrel *et al.* 2007; Moseley *et al.* 2007). Heterozygous $\alpha3^{+/-}$ mice are slower learners and more 'manic' than wild-type mice, but they, too, have reduced long-term memory (Lingrel *et al.* 2007; Moseley *et al.* 2007). Mice with genetically dysfunctional $\alpha3$ Na^+ pumps also exhibit 'mania-like' behaviour (Kirshenbaum *et al.* 2011).

Mice with mutated, ouabain-resistant, but otherwise functional $\alpha2$ Na^+ pumps ($\alpha2^{R/R}$ mice) exhibit decreased locomotor activity in novel environments and have a blunted, non-habituating auditory startle reflex (Schaefer *et al.* 2011). $\alpha2^{R/R}$ mice have normal spatial learning and memory, but are hyper-responsive to stimulation by methamphetamine, a sympathomimetic that enhances dopamine-mediated behaviour. These studies and others on $\alpha2^{R/R}$ mice (Dostanic *et al.* 2005; Dostanic-Larson *et al.* 2005) demonstrate the physiological importance of the ouabain binding site and imply that an endogenous ligand binds to this site and regulates $\alpha2$ Na^+ pump function.

Intracerebroventricular infusion of ouabain in rats increases locomotor activity (El-Mallakh *et al.* 2003) and augments expression of $\alpha2$ in the basal ganglia and $\alpha3$ in the frontal cortex (Hamid *et al.* 2009). The ouabain-induced hyperactive behaviour is antagonized

by anti-manic agents (El-Mallakh *et al.* 2003, 2006). Moreover, several reports have linked bipolar mood disorders in humans to reduced Na^+ pump activity (Looney & el-Mallakh, 1997), to reduced expression of $\alpha2$ or $\alpha3$ Na^+ pumps (Rose *et al.* 1998) or to an endogenous ouabain-like compound (Goldstein *et al.* 2006, 2011). This is additional evidence that ouabain and some other cardiotonic steroids (CTS) are endogenous to mammals (Hamlyn *et al.* 1991; Schoner & Scheiner-Bobis, 2007; Blaustein *et al.* 2012).

Many investigators have studied the effects of ouabain and related CTS on the brain, but most have used relatively high (micromolar) concentrations. For example, in rat hippocampal slices, 20 μM dihydro-ouabain (DHO) induces neuronal hyperexcitability and a form of long-term depression (Vaillend *et al.* 2002; Reich *et al.* 2004). In rat cortical slices, 20–100 μM ouabain or DHO depolarizes both fast-spiking interneurones and pyramidal cells (Anderson *et al.* 2010). These high CTS concentrations block rodent $\alpha1$ Na^+ pumps as well as $\alpha2$ Na^+ pumps (O'Brien *et al.* 1994). In contrast, nanomolar ouabain, which inhibits $\alpha2$ and $\alpha3$, but not rodent $\alpha1$ pumps, was used in one study, in which application of 10 nM ouabain to mouse hippocampal slices for 2 min depolarized inhibitory interneurones by ~7 mV and thereby increased spontaneous inhibitory postsynaptic potential frequency in pyramidal cells (Richards *et al.* 2007). The authors concluded that Na^+–K^+ homeostasis was regulated by $\alpha3$ Na^+ pumps in interneurones but by $\alpha1$ Na^+ pumps in pyramidal cells, which were depolarized by 25 but not 10 nM ouabain (Richards *et al.* 2007).

In order to gain a better understanding of the role of high-ouabain-affinity Na^+ pumps in neurones, we examined the effects of nanomolar ouabain on Ca^{2+} signalling evoked by L-glutamate (Glu) and carbachol (CCh) in primary cultured hippocampal neurones in rat neurone–glia co-cultures. This simplified system was used on the assumption that the properties and activity of specific Na^+ pump isoforms are comparable in the cultured cells and in more intact preparations, as we observed in arterial smooth muscle (Zhang *et al.* 2005; Song *et al.* 2006).

Methods

Primary neurone–glia co-cultures

All animal protocols were approved by the University of Maryland School of Medicine Institutional Animal Care and Use Committee and conformed to the principles of UK regulations. The pregnant (18 days) Sprague–Dawley rat dams were killed by CO_2 asphyxiation followed by thoracotomy, and the fetuses were removed and killed by decapitation. Hippocampal neurone–astrocyte co-cultures were prepared from the fetuses on embryonic day 18. The hippocampus was isolated in Hank's balanced salt solution (HBSS; Lonza, Allendale, NJ, UK) supplemented with 0.3% bovine serum albumin and 10 mM $MgSO_4$ ('HBSS+'). The tissue was dissociated in HBSS+ with 0.25% trypsin–EDTA (Invitrogen, Carlsbad, CA, USA). Dissociated cells were collected by centrifugation at 500 g, for 1 min and cultured on poly-L-lysine-coated 25 mm glass coverslips with Neurobasal culture medium supplemented with B-27, 0.01% glutaMAX, 5% fetal bovine serum (all from Invitrogen) and 1 μg ml^{-1} gentamicin (Lonza) and maintained for 7–14 days (37°C in air supplemented with 5% CO_2); the cells were fed twice weekly with culture medium without fetal bovine serum.

Immunocytochemistry

Coverslips containing the co-cultured neurones and astrocytes were fixed with 4% paraformaldehyde and then permeabilized with 0.5% Brij 58 Sigma-Aldrich (St Louis, MO, USA) (10 min, 20–25°C). The cells were stained with isoform-specific rabbit polyclonal antibodies raised against the Na^+ pump $\alpha1$, $\alpha2$ and $\alpha3$ catalytic subunits (sequences 'NASE', 'HERED' and 'TED', respectively; Pressley, 1992). Chicken anti-neurofilament-H (anti-NF-H) and rabbit anti-glial fibrillary acidic protein (anti-GFAP) antibodies (Neuromics, Edna, MN, USA) were used to label the neurones and astrocytes, respectively. Nuclei were stained with 4′,6′-diamidino-2-phenylindole (DAPI) (0.5 μg ml^{-1}; Invitrogen). Details of our immunocytochemical methods are published (Song *et al.* 2006). Images were acquired with a Nikon Diaphot inverted microscope (Nikon Corporation, Melville, NY, USA) equipped with a long working distance PlanApo 60× (n.a. 1.2; water immersion) objective, or a Zeiss LSM 410 laser scanning confocal microscope (Carl Zeiss Microscopy, Thornwood, NY, USA) with a planApo 63× (n.a. 1.4; oil) objective. Images were analysed with Meta Imaging System software (Molecular Devices, West Chester, PA, USA); details are published (Lee *et al.* 2006; Song *et al.* 2006).

Ca^{2+} signalling

For live cell imaging, cells on coverslips were loaded (45 min) with 3 μM fura-2 (Invitrogen) in physiological salt solution (PSS; pH 7.4; 20–25°C) and were imaged at 35°C in a custom superfusion chamber (0.22 ml) filled with PSS. Pharmacological reagents were added to the PSS (see Results). The superfusion rate was 2 ml min^{-1} with a gravity-fed perfusion system (Warner Instruments, Hamden, CT, USA); the dead time in the system was 4 s. Cells were superfused with control PSS for 15–20 min at

the start of each experiment to wash out extracellular fura-2 and obtain a stable baseline.

Cells were imaged with a Nikon Eclipse 2000 inverted microscope equipped with a UV-Fluor 40× (n.a. 1.4; oil) objective lens (Nikon) and recorded with a Hamamatsu ORCA-ER CCD camera (Hamamatsu Photonics, Bridgewater, NJ, USA). A Lambda DG-4 wavelength switcher with a xenon arc lamp (Sutter Instruments, Novato, CA, USA) provided illumination. Wavelengths used for fura-2 are as follows: excitation at 360 and 380 nm, where 360 nm is the isosbestic point; and emission at 535 nm. Acquired images were analysed using a Meta Imaging System (Molecular Devices). Details of our methods are published (Golovina *et al.* 2003; Lee *et al.* 2006).

To avoid artifacts due to variations in Ca^{2+} concentration calibration in different cells and cell types and in the presence of various drugs, we used the fluorescence emission ratio with the two excitation wavelengths ('fura-2 ratio', F_{360}/F_{380}) as a measure of the cytosolic Ca^{2+} concentration ($[Ca^{2+}]_i$). The rate of image capture was varied during the experiments. When stimuli such as L-glutamate were applied, the capture rate was approximately three ratio images per second; in resting or washout conditions, the capture rate was reduced to one ratio image every 20 or 30 s. For statistical analysis of the changes in evoked increases in the fura-2 ratio, i.e. $\Delta F_{360}/F_{380}$, the ratio in basal (resting) conditions was subtracted from the peak F_{360}/F_{380} evoked by stimulation with ATP, Glu or low Na^+ medium, as follows:

$$\Delta F_{360}/F_{380} = (\text{peak} F_{360}/F_{380}) - (\text{basal} F_{360}/F_{380})$$

Relatively low-magnification images were studied in most experiments, so that data could be obtained from many cells (both astrocytes and neurones) simultaneously. In these circumstances, the Ca^{2+} signals in most neuronal processes are difficult to measure. In order to compare the signals in the axon and dendrites with those in the cell soma, we also analysed magnified images in some experiments.

Solutions and reagents

The composition of the PSS used for experiments was as follows (mM): 140 NaCl, 5 KCl, 1.8 $CaCl_2$, 1.4 $MgCl_2$, 5 $NaHCO_3$, 1.2 NaH_2PO_4, 11.5 glucose and 10 Hepes (pH 7.4). In Ca^{2+}-free (0Ca) PSS, the 1.8 mM $CaCl_2$ was omitted and 0.1 mM EGTA was added. In the low-Na^+ PSS, the 140 mM NaCl was replaced by 140 mM LiCl. All salts and other reagents were 'reagent grade' or the highest purity available. The following reagents were purchased from Tocris (Ellisville, MO, USA): CCh (carbamoylcholine or carbachol), D-AP5 (2-amino-5-phosphopentanoic acid), LY341495 [(2*S*)-2-amino-2-((1*S*,2*S*)-2-carboxycycloprop-1-yl)-3-(xanth-9-yl)-propanoic acid], LY367385 [(*S*)-(+)-α-amino-4-carboxy-2-methylbenzeneacetic acid] and MPEP [2-methyl-6-(phenylethynyl)-pyridine]. All other reagents were obtained from Sigma-Aldrich (St Louis, MO, USA).

Statistical methods

Averaged data are presented in terms of the fura-2 ratios in '*n*' individual cells. Only data from cells that could be clearly identified as neurones or astrocytes on the basis of their responses to L-glutamate and ATP (see Results) are reported. Unless noted in the figure legends, all averaged data come from three or more coverslips from at least two different cell cultures. Comparisons are based on changes in the fura-2 ratio (i.e. changes in $[Ca^{2+}]_i$) in individual cells in different conditions. Individual cell data were included in the statistics when the peak 'control' responses (e.g. to Glu) at the end of the experiment were comparable to those at the start. Statistical analyses were performed with one-way ANOVA and a Bonferroni *post hoc* test, as indicated in the figure legends; $P < 0.05$ was considered a significant difference. Dose–response data were fitted to the Hill equation. Time course data were fitted to a four-parameter logistic curve with SigmaPlot 11.0 software (Systat Software, Inc., San Jose, CA, USA).

Results

Expression of high-ouabain-affinity Na^+ pump (α2 and α3) catalytic subunits in cultured neurones and glia

All of the cells (identified by DAPI-stained nuclei; blue) in the rat hippocampal neurone–glia co-cultures cross-reacted with either anti-NF-H (green) or anti-GFAP (red) antibodies (Fig. 1*A*). Thus, the cultures appear to be pure neurone–glia co-cultures. Moreover, most of the glia appear to be type 2 astrocytes on the basis of their stellate structure and round nuclei (Yarowsky & Krueger, 1989).

To identify the high-ouabain-affinity receptors (α2 or α3 Na^+ pumps), the cultured cells were cross-reacted with antibodies raised against the α2 or α3 catalytic subunit (Pressley, 1992) and with anti-NF-H (Fig. 1*B* and *C*). All NF-H-positive cells (i.e. neurones) cross-reacted with anti- α3, but not anti-α2 (Fig. 1*B*). In contrast, all NF-H-negative cells (presumably astrocytes; see Fig. 1*A*) cross-reacted with anti-α2, but not anti-α3 (Fig. 1*C*). A higher magnification confocal image (Fig. 1*D*) shows that the α3 labelling is punctate and is confined to the surface of the cell body (in this image plane through the cell

body), the axon and the dendrites. Thus, all of these hippocampal pyramidal-shaped neurones, as well as other types of neurones, express α3 ('N' in Fig. 1*B*) and α1 Na^+ pumps (Fig. 1*E*); in contrast, all astrocytes express α2 ('A' in Fig. 1*C*) and α1 Na^+ pumps (Juhaszova & Blaustein, 1997*b*; Song *et al.* 2006). In both neurones and astrocytes, the α1 pumps are ubiquitously distributed over the cell surface (e.g. Fig. 1), with no evidence of the reticular distribution that is characteristic of α2 and α3 pumps (Juhaszova & Blaustein, 1997*a*).

Responses of co-cultured neurones and astrocytes to glutamate and ATP

Numerous reports indicate that both neurones and astrocytes respond to stimulation by Glu and ATP or adenosine (van den Pol *et al.* 1992; Araque *et al.* 2001; Halassa & Haydon, 2010). In order to perform Ca^{2+} imaging studies of neuronal function in neurone–glia co-cultures, it is imperative to distinguish these two cell types. Therefore, the effects of bath-applied Glu and ATP on Ca^{2+} signalling were studied in fura-2-loaded, co-cultured cells on coverslips (Fig. 2*A*). Immediately after the Ca^{2+} imaging experiment, the cells on the coverslip were fixed and immunostained (Fig. 2*B*) in order to identify the neurones (NF-stained cells; green) and astrocytes (GFAP-stained cells; red). Figure 2*C* shows the time course of the responses of one neurone and one astrocyte (cells 'N' and 'A', respectively) to the application of ATP and Glu. Figure 2*Da–d* illustrates the relative $[Ca^{2+}]_i$ (shown as the fura-2 F_{360}/F_{380} ratio images) in resting conditions (Fig. 2*Da*) and during the application of ATP (Fig. 2*Db*) and Glu (Fig. 2*Dc* and *d*); the times of image acquisition are indicated by arrows *a–d* in Fig. 2*C*. ATP (0.5 μM) elicited a Ca^{2+} transient only in the astrocytes (Fig. 2*C* and *Db*). When the coverslip was superfused with medium containing 4 μM Glu, only the neurones exhibited a Ca^{2+} transient initially (Fig. 2*C* and

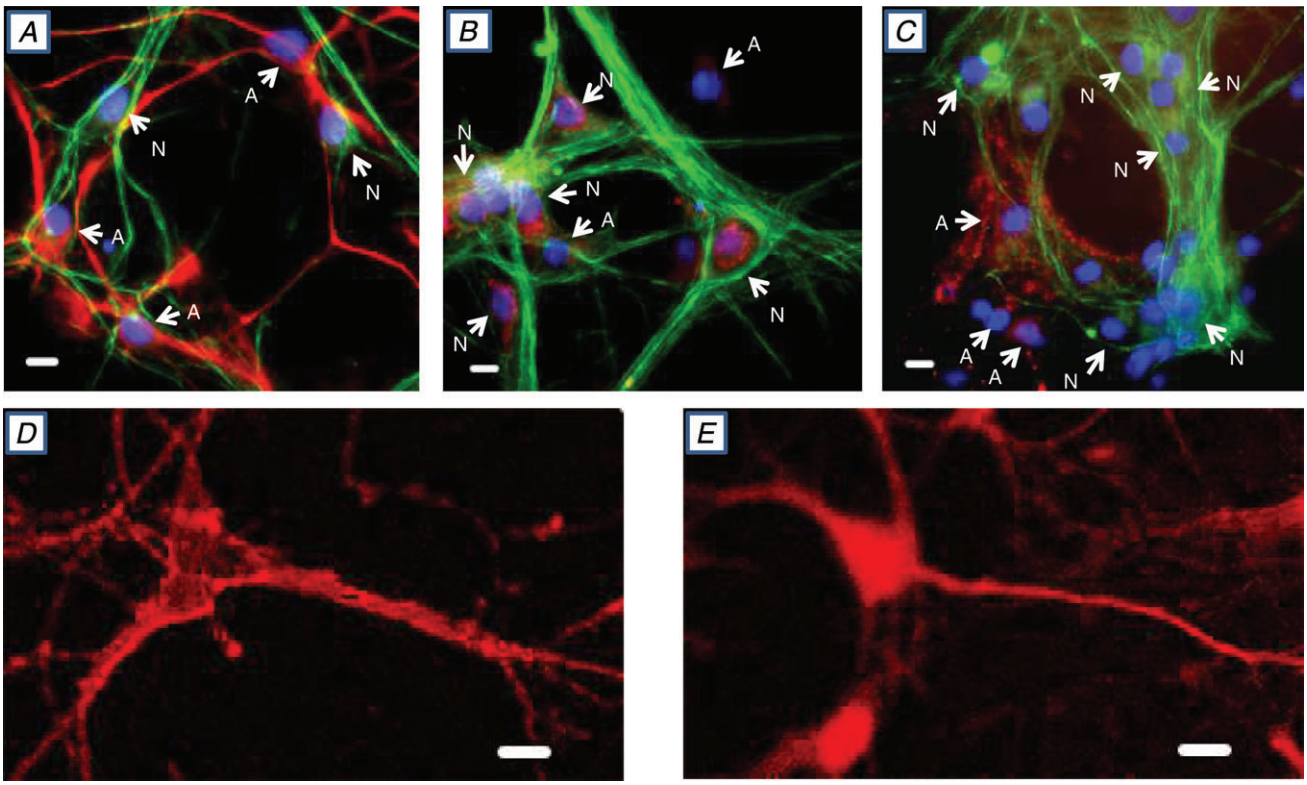

Figure 1. Identification of neurones and astrocytes, and location of Na^+ pump α1, α2 and α3 subunits, in rat hippocampal neurone–astrocyte co-cultures
A, all cells, identified by DAPI-stained nuclei (blue), cross-reacted with either anti-neurofilament-H (anti-NF-H) antibodies (N = neurones, green) or anti-glial fibrillary acidic protein (anti-GFAP) antibodies (A = astrocytes, red). *B*, all neurones (N = NF-H-positive cells, green, with blue, DAPI-stained nuclei) cross-reacted with anti-α3 antibodies (TED, red). No astrocytes (A = NF-H-negative cells with DAPI-stained nuclei) cross-reacted with anti-TED antibodies. *C*, astrocytes (A = NH-F-negative cells with DAPI-stained nuclei), but no neurones (N = NH-F-positive green cells with DAPI-stained nuclei), cross-reacted with anti-α2 antibodies (HERED, red). *D* and *E*, confocal images of neurones cross-reacted with anti-α3 antibodies (*D*; TED, red) and anti-α1 antibodies (*E*, NASE, red). The data in all panels are each representative of at least 4 or 5 similar preparations. Scale bars in *A–E* represent 20 μm.

Dc), but some astrocytes also responded with a smaller, delayed transient (Fig. 2*C* and *Dd*).

In most subsequent studies, we used similar low concentrations of Glu and ATP, in order to distinguish between neuronal and astrocyte responses without having to immunostain the cells. In a few experiments, however, a range of concentrations of Glu (1–10 μM) and ATP (0.5–10 μM) were tested (data not shown). When the higher Glu and ATP concentrations ($\geq$5 μM) were tested, both cell types usually responded to both agents, as reported by van den Pol *et al.* (1992). In contrast, some, but not all, astrocytes responded to low-dose (3–4) μM Glu; when they did respond to 3–4 μM Glu, however, the astrocyte Ca^{2+} signals were typically smaller and delayed in comparison to the neuronal responses (Fig. 2*C* and *Dd*). We cannot rule out the possibility that the delayed response is a consequence of evoked neuronal release of ATP or adenosine (Verderio & Matteoli, 2011).

Pharmacology of the Glu-induced Ca^{2+} signals

Are the neuronal responses to bath-applied Glu initiated by the activation of ionotropic, Ca^{2+}-permeable receptors (NMDARs) or by metabotropic Glu receptors (mGluRs)? To address this question, we tested the effects of the reversible NMDAR and mGluR antagonists, AP5 (Riaza Bermudo-Soriano *et al.* 2012) and LY341495 (Zhu *et al.* 2005), respectively (Fig. 3). The Glu-evoked Ca^{2+} transients were unaffected by 80 μM AP5 (Fig. 3*A*) or by 1 μM LY341495 (data not shown), which should inhibit group II mGluRs (Kingston *et al.* 1998). The Ca^{2+} transients were, however, inhibited by ~50% by 10 μM LY341495 (Fig. 3*B*), which blocks most mGluRs (Kingston *et al.* 1998). DMSO (0.33%), the diluent used for 10 μM LY341495, had no effect on the Glu-evoked Ca^{2+} signals (Fig. 3*B*), but higher LY341495 concentrations were not tested because 1% DMSO, itself, significantly reduced the response to Glu (not shown).

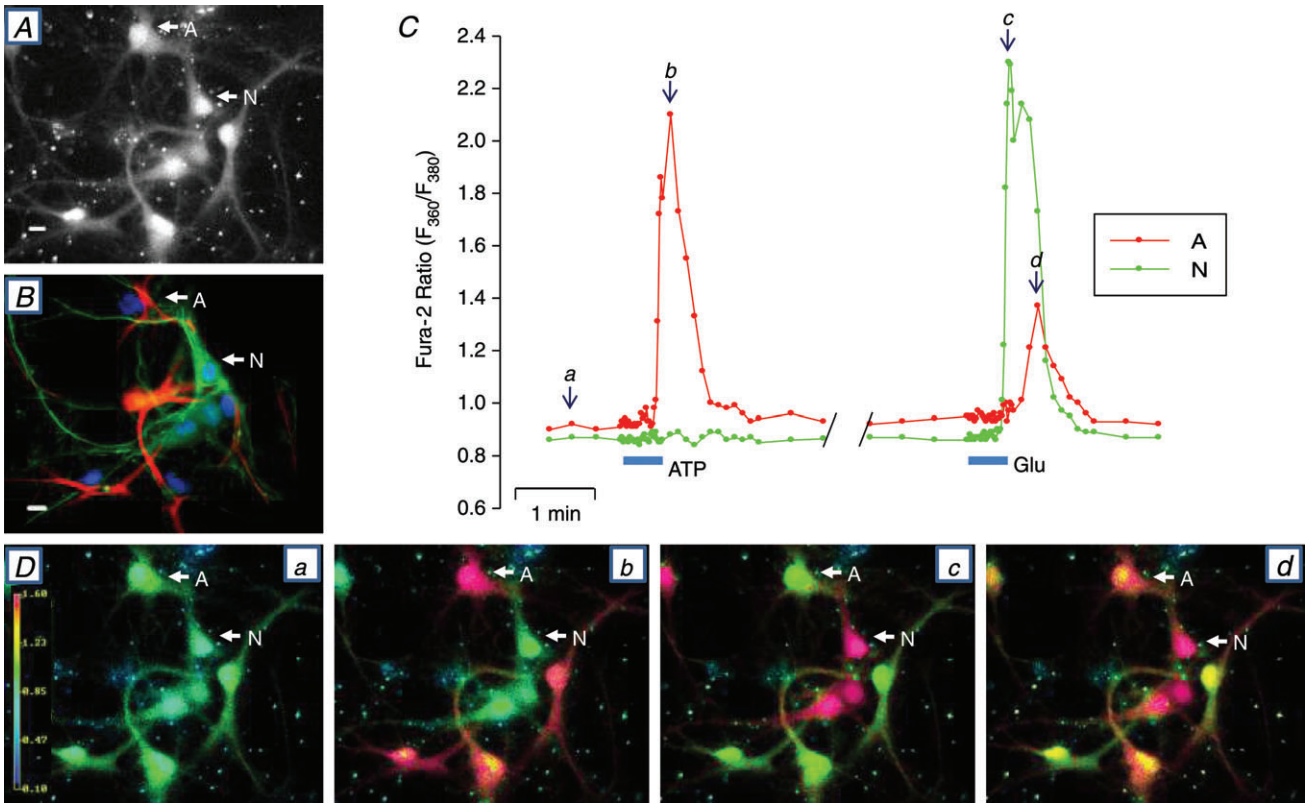

Figure 2. ATP- and Glu-evoked Ca^{2+} signals in neurones and astrocytes in a rat hippocampal neurone–astrocyte co-culture
A, fura-2 stained neurones and astrocytes (F_{360} excitation) immediately before initiating the Ca^{2+} signalling experiment. Cell A is an astrocyte and N is a neurone. *B*, immunostained cells from the same field as in *A*. Immediately after the Ca^{2+} signalling experiment, the cells on the coverslip were fixed and cross-reacted with anti-NF-H antibodies to identify neurons (N, green) and with anti-GFAP antibodies to identify astrocytes (A, red). All nuclei were stained with DAPI. *C*, time course of changes in the fura-2 F_{360}/F_{380} ratio, illustrating the effects of 0.5 μM ATP and 4 μM L-glutamate (Glu). *D*, fura-2 F_{360}/F_{380} ratio images captured at time points *a*–*d* indicated in *C*. These data are a representative example of 4 similar, fully analysed experiments.

Two group I mGluR antagonists, LY367385, which selectively blocks mGluR1, and MPEP, which blocks mGluR5 (Mannaioni *et al.* 2001), were tested. The 3 μM Glu-evoked Ca^{2+} signal was unaffected by 100 μM LY367385, but was markedly reduced by 3 and 10 μM MPEP (Fig. 4). Thus, the neuronal responses to Glu stimulation appear to be mediated by mGluR5; they are not mediated by ionotropic receptors or by mGluR1 or mGluR2.

Effects of low-dose cardiotonic steroids on Ca^{2+} signals in neurones

Cardiotonic steroids, such as ouabain and digoxin, which inhibit Na^+ pumps, enhance Ca^{2+} signalling in many types of cells. Such experiments are often performed with micromolar or higher concentrations of CTS (Vaillend *et al.* 2002; Reich *et al.* 2004; Anderson *et al.* 2010) which, even in rodents, inhibit α1 as well as α2 or α3 Na^+ pumps

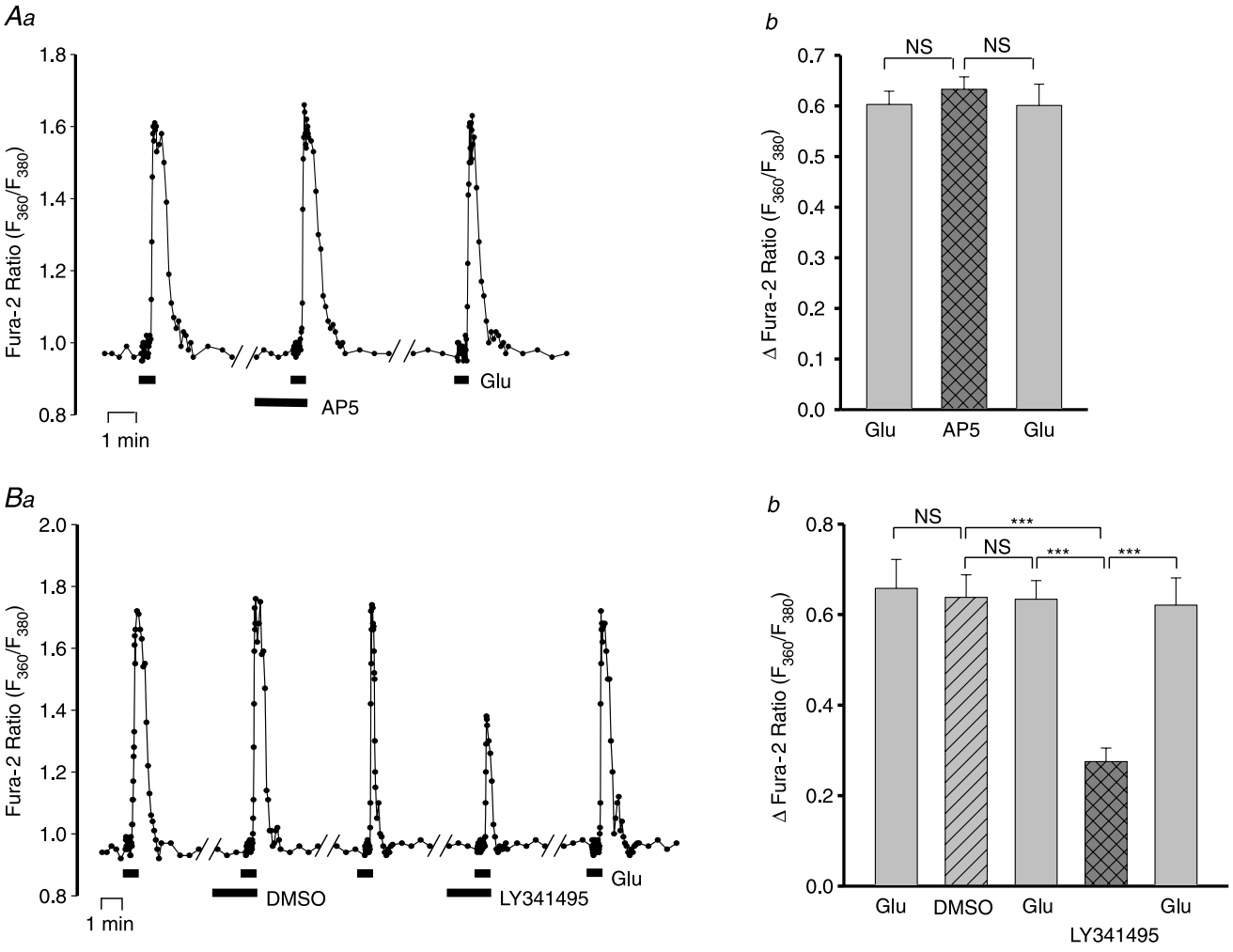

Figure 3. Effects of the glutamate receptor blockers, AP5 and LY341495, on neuronal Ca^{2+} signals evoked by bath-applied Glu in rat hippocampal neurone–astrocyte co-cultures
A, effect of 80 μM AP5 on the Ca^{2+} signals evoked by 4 μM Glu. *Aa*, fura-2 F_{360}/F_{380} ratio data from a representative neurone. There was a 5 min washout in control physiological saline solution (PSS) between each of the data segments shown. Note that the frequency of image capture was increased to 3 ratios s^{-1} during the periods of exposure to Glu. *Ab*, averaged maximal Glu-evoked increase in the fura-2 ratio ($\Delta F_{360}/F_{380}$) before, during and after exposure to 80 μM AP5; $n = 25$ neurones. The effect of AP5 on the peak response was not significantly different (NS) from the control responses (ANOVA). *B*, effect of 10 μM LY341495 on the Ca^{2+} signals evoked by 4 μM Glu. *Ba*, fura-2 F_{360}/F_{380} ratio data from a representative neurone. In these experiments, the effect of the LY341495 diluent, DMSO (0.33%), was also tested on the response to Glu (see *Aa*, above, for additional details). *Bb*, averaged maximal increase in $\Delta F_{360}/F_{380}$ before, during and after treatment with 0.33% DMSO and 10 μM LY341495 in 0.33% DMSO; $n = 27$ neurones. $^{***}P < 0.001$; NS, not significant for the indicated pairs (ANOVA).

(O'Brien *et al.* 1994). The enhancement of Ca^{2+} signals by CTS is widely believed to result from inhibition of Na^+ pumps and the consequent rise in (local) cytosolic Na^+ concentration ($[Na^+]_i$) The increased $[Na^+]_i$ promotes net Ca^{2+} gain via Na^+–Ca^{2+} exchangers (Blaustein & Wiesmann, 1970; Blaustein, 1993; Blaustein & Lederer, 1999), which co-localize with, and functionally couple with, $\alpha 2$ or $\alpha 3$ Na^+ pumps in astrocytes and neurones, respectively (Juhaszova & Blaustein, 1997*a*; Song *et al.* 2006). Incubation with 3 nM ouabain or 10 nM digoxin for up to 10 min had no detectable effect on the fura-2 ratio in unstimulated cells (i.e. 'resting' or basal $[Ca^{2+}]_i$). Nevertheless, neuronal Ca^{2+} transients evoked by 3 μM Glu were substantially amplified when the cells were pre-incubated with 10 nM digoxin or 3 nM ouabain (Fig. 5*Aa* shows representative data from one cell; Fig. 5*Ab* shows summary data). The CTS-induced increment in the response (Δfura-2 ratio) was CTS concentration dependent. The ouabain dose–response data fitted the Hill equation with a Hill coefficient of 1, indicating no ligand co-operativity, and apparent $EC_{50} = 0.5$ nM (Fig. 5*B*). The digoxin dose–response curve was not explicitly investigated, but the EC_{50} for digoxin also appeared to be of the order of 1 nM (data not shown).

The relative magnitude of the increment depended upon the duration of the pre-incubation with ouabain. Figure 5*C* shows that the effect of ouabain was rapid; a 1 min pre-incubation with 3 nM ouabain was sufficient to amplify, significantly, the neuronal response to 3 nM Glu. The time course curve (Fig. 5*C*) indicates that a 50 s

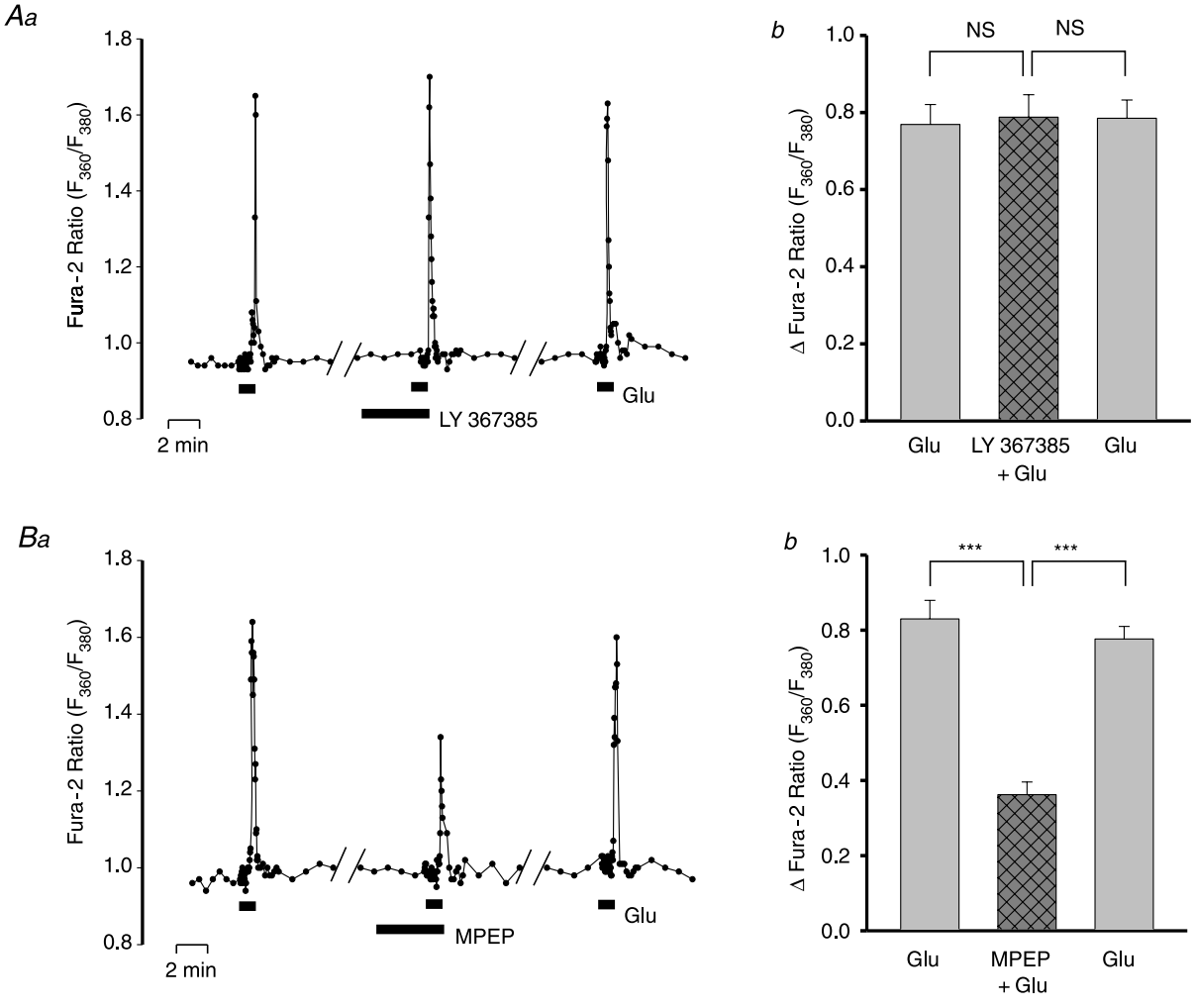

Figure 4. Effects of inhibitors of group II glutamate receptors, LY367385 and MPEP, on the neuronal Ca^{2+} signals evoked by bath-applied Glu
A, effect of 100 μM LY367385 on the F_{360}/F_{380} ratio signal evoked by 3 μM Glu. *Aa*, data from a representative neurone. *Ab*, summarized data from 26 neurones. NS, no significant difference. *B*, effect of 3 μM MPEP on the F_{360}/F_{380} ratio signal evoked by 3 μM Glu. *Ba*, data from a representative neurone. *Bb*, summarized data from 36 neurones tested with 5 or 10 μM MPEP. The 5 and 10 mM MPEP results were combined because there was negligible difference between the effects of the two doses when both were tested in the same cells. ***$P < 0.001$ *vs.* Glu-evoked responses pre- and post-MPEP (ANOVA).

pre-incubation with 3 nM ouabain yielded a half-maximal effect; a 5 min exposure to ouabain, the time used for most experiments, produced a near-maximal augmentation of the Glu-evoked Ca^{2+} transient.

The relative magnitude of the amplification by ouabain also depended upon the magnitude of the initial response to Glu (not shown). When 3 μM Glu was used, and the Glu-evoked Ca^{2+} transients were relatively small, 3 nM ouabain greatly augmented the transients. When 5 μM Glu was used, however, the Ca^{2+} transients were much larger, and the relative amplification by 3 nM ouabain was then much smaller, probably

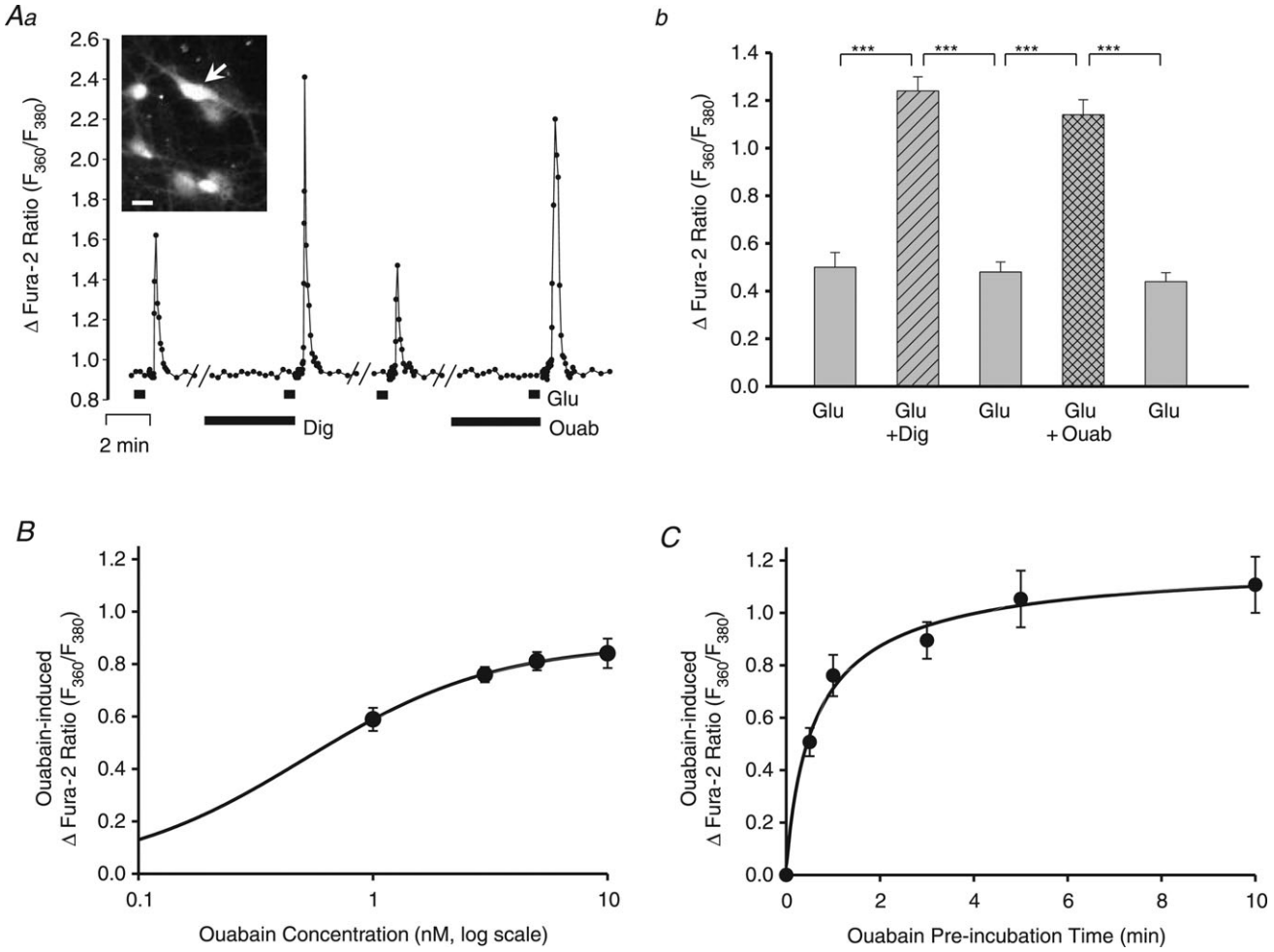

Figure 5. Effects of nanomolar concentrations of cardiotonic steroids on Glu-evoked Ca^{2+} signals in neurones in rat hippocampal neurone–astrocyte co-cultures
A, effects of 10 nM digoxin (Dig) and 3 nM ouabain (Ouab) on the F_{360}/F_{380} ratio signal evoked by 3 μM Glu. *Aa*, data from a representative neurone (arrow in inset shows an F_{360} fura-2 image of this cell sitting on an astrocyte). The diluent for the digoxin was DMSO (final concentration of 0.33%); ouabain is water soluble. The cells were pre-incubated with digoxin or ouabain for 5 min before the stimulation with 3 μM Glu. There was a 13–14 min washout period between each of the records shown. *Ab*, summary data for 14 cells like the one in Fig. 5*A*, in which 10 nM digoxin and 3 nM ouabain were both tested. ***$P < 0.001$ *vs.* control 'before' and 'after' responses to 3 μM Glu alone (ANOVA). *B*, ouabain log dose–response curve. The cells were pre-incubated with ouabain for 5 min before the stimulation with 3 μM Glu. The lowest ouabain concentration tested in these experiments was 1 nM. Each data point is the mean ± SEM of the ouabain-induced Δfura-2 ratio (ΔF; i.e. the difference between the peak F_{360}/F_{380} in Glu alone and in Glu + ouabain; see *Aa*) from 44–69 neurones, from a total of 8 experiments. The data were fitted to the Hill equation, $\Delta F/\Delta F_{max} = [Ouab]^n/(EC_{50} + [Ouab]^n)$, with the following parameters: $\Delta F_{max} = 0.89$, the ouabain $EC_{50} = 0.5$ nM, and the Hill coefficient, n, = 1; [Ouab] is the ouabain concentration tested. This EC_{50} (0.5 nM) is comparable to the EC_{50} for ouabain on $\alpha 2$ Na^+ pumps in rat arterial smooth muscle (Raina *et al.* 2010). *C*, effect of the duration of pre-incubation with 3 nM ouabain on the $\Delta F_{360}/F_{380}$ evoked by 3 μM Glu (i.e. the ouabain-induced Δfura-2 ratio; see *B*). Each data point is the mean ± SEM of data from 18–45 neurones, from a total of 10 experiments. The pre-incubation time for a half-maximal response to 3 nM ouabain, 50 s, was determined from the empirical single binding site curve.

because peak $[Ca^{2+}]_i$ was already near saturation before the application of ouabain.

The aforementioned results refer to the signals in the cell soma. To determine whether similar effects occurred in the cell processes, higher magnification images were examined. Figure 6 shows that the Glu-evoked Ca^{2+} signals in the axon and dendrites also were augmented by 3 nM ouabain. Thus, this effect is not limited to the soma; the mechanism appears to function throughout the neuron.

Responses of neurones to serotonin and carbachol, and the effects of ouabain

In order to be certain that the effects of ouabain were not specific for Glu-evoked Ca^{2+} transients, we also examined the responses to two other agonists, serotonin (5-HT) and the acetylcholine receptor agonist, CCh. The cultured hippocampal neurones did not respond to 10–15 μM 5-HT (data not shown). The neurones, but not astrocytes, did, however, exhibit Ca^{2+} transients in response to 3 and 10 μM CCh (Fig. 7); i.e. CCh elicited Ca^{2+} transients only in Glu-responsive, and not in ATP-responsive cells. The CCh-evoked Ca^{2+} transients, which were presumably mediated by metabotropic muscarinic receptors (Sohn *et al.* 2007; Zhang & Seguela, 2010), also were significantly augmented by 3 nM ouabain (Fig. 7).

Mechanisms underlying the augmentation of the neuronal Ca^{2+} transients

A critical question is, what mechanism(s) is (are) responsible for this CTS-induced augmentation of the Glu-evoked Ca^{2+} signals? Is it increased Ca^{2+} release from ER stores and/or net Ca^{2+} gain mediated by NCX? This is addressed in the following sections.

Modulation of ER Ca^{2+} stores by ouabain. To determine whether ouabain affects the neuronal ER Ca^{2+} stores, the Ca^{2+} transients evoked by 10 mM caffeine (CAF) plus 10 μM cyclopiazonic acid (CPA) were measured before and after a 4 min pretreatment with ouabain. Caffeine opens ER ryanodine receptors, while CPA blocks the ER Ca^{2+} pump (SERCA) and may increase the leak of Ca^{2+} from the ER (Blaustein & Golovina, 2001). The CAF and CPA were administered in Ca^{2+}-free medium to eliminate Ca^{2+} entry via store-operated channels (Koss *et al.* 2009) and other pathways. Pre-incubation with 3 nM ouabain increased the amplitude of the CAF + CPA-evoked Ca^{2+} transient by ~25% (Fig. 8). The use of Ca^{2+}-free medium may even

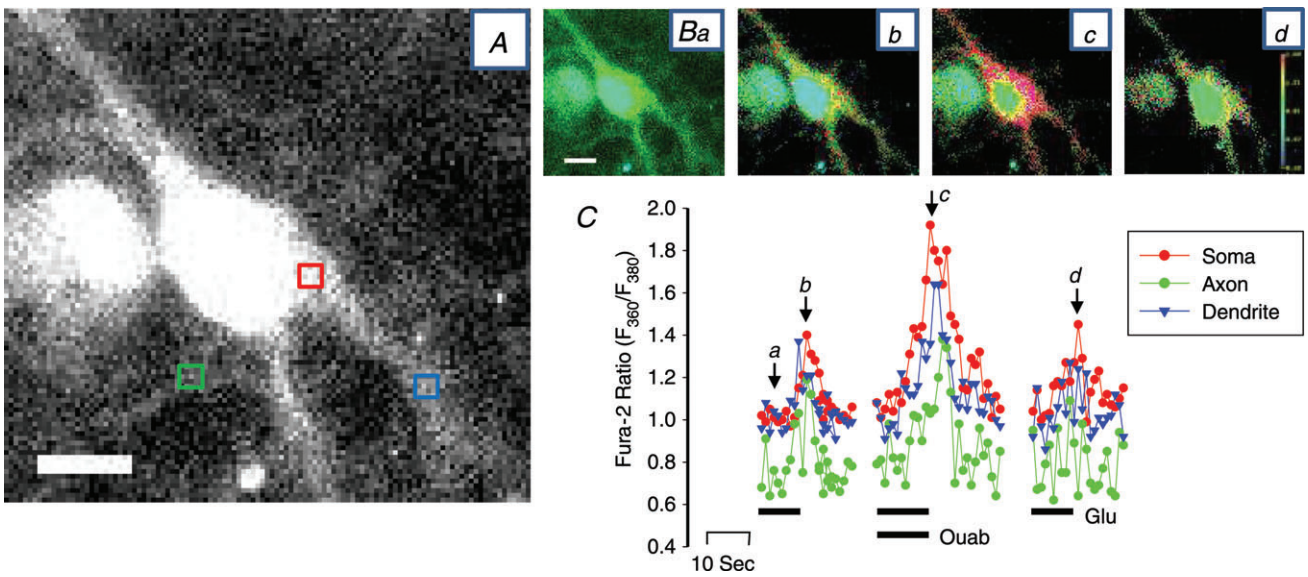

Figure 6. Effects of nanomolar ouabain on Ca^{2+} signals in axons and dendrites
A, enlarged fura-2 (F_{380}) image of a neurone showing the areas from which the time course data in *C* were obtained; the soma (red box), the axon (green box) and a dendrite (blue box) are indicated. The contrast was enhanced in this image to help visualize the axon. *B*, F_{360}/F_{380} ratio images obtained in basal conditions (*Ba*), at the peak of the first response to 3 μM Glu (*Bb*), at the peak of the response to 3 nM ouabain + 3 μM Glu (*Bc*) and at the peak of the response to Glu after washout of ouabain (*Bd*). *C*, time course of the Ca^{2+} transients (F_{360}/F_{380} ratios) recorded within the red, green and blue boxes in *A* (soma, axon and dendrite, respectively). The protocol was the same as that used in Fig. 5*Aa*; only the periods before, during and after the Glu-evoked transients are shown. Lettered arrows indicate the times at which images *Ba–d* were recorded. This neurone is representative of more than 10 neurones in which this type of analysis was performed. Similar results were obtained with digoxin (e.g. in the neurone indicated by the arrow in the inset in Fig. 5*Aa*). Calibration bars in *A* and *Ba* represent 20 μM.

have attenuated the effect because prolonged exposure to Ca^{2+}-free medium itself depletes the ER Ca^{2+} stores (data not shown). These results indicate that ouabain increased the releasable pool of Ca^{2+} stored in the neuronal ER. The data are consistent with the view that nanomolar ouabain augments Glu-evoked Ca^{2+} transients in the neurones by reducing the Na^+ electrochemical gradient across the PM at PM–ER junctions. In turn, this drives Ca^{2+} into the cells via NCX and thereby promotes enhanced ER Ca^{2+} storage.

Role of NCX in the action of ouabain. To verify the role of NCX in the ouabain-induced augmentation of Ca^{2+} signalling, we employed the NCX antagonist, SEA0400 (Annunziato *et al.* 2004; Iwamoto *et al.* 2007). In control experiments, SEA0400 (300 nM) had no effect on the amplitude of 3 μM Glu-evoked Ca^{2+} transients (Fig. 9*A*), but it virtually abolished the ouabain-induced augmentation of the transients (Fig. 9*B*). These results support the view that the ouabain-induced increase in ER Ca^{2+} store content and the augmented

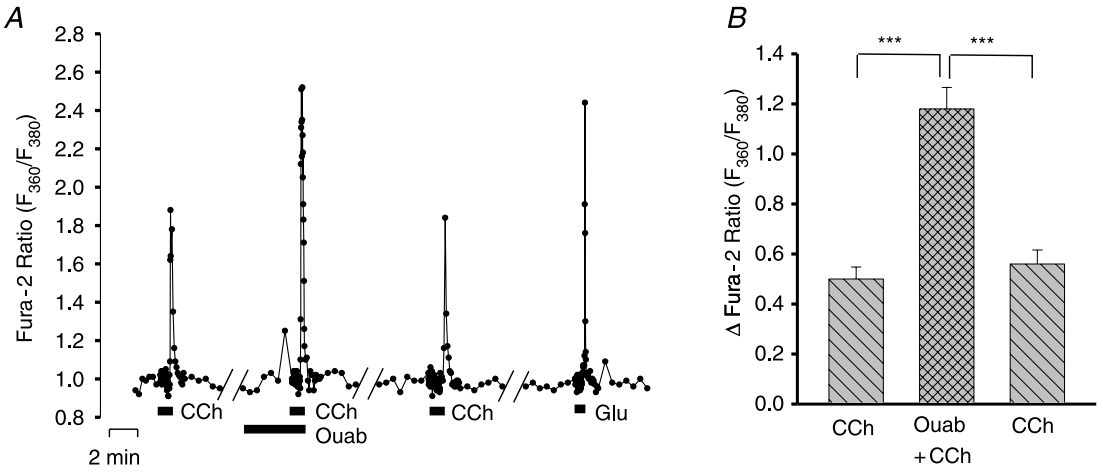

Figure 7. Effects of nanomolar ouabain on Ca^{2+} signals evoked by bath-applied carbachol (CCh) in neurones
A, F_{360}/F_{380} ratio data from a representative neurone in which the effect of 3 nM ouabain was tested on the Ca^{2+} transient evoked by 3 μM CCh. All the CCh-responsive cells also responded to 3 μM Glu; none responded to 0.5 μM ATP (not shown). *B*, summary data for 42 cells like the one in *A*, in which the effects of 3 nM ouabain were tested. ***$P < 0.001$ *vs.* control 'before' and 'after' responses to 3 μM CCh alone (ANOVA).

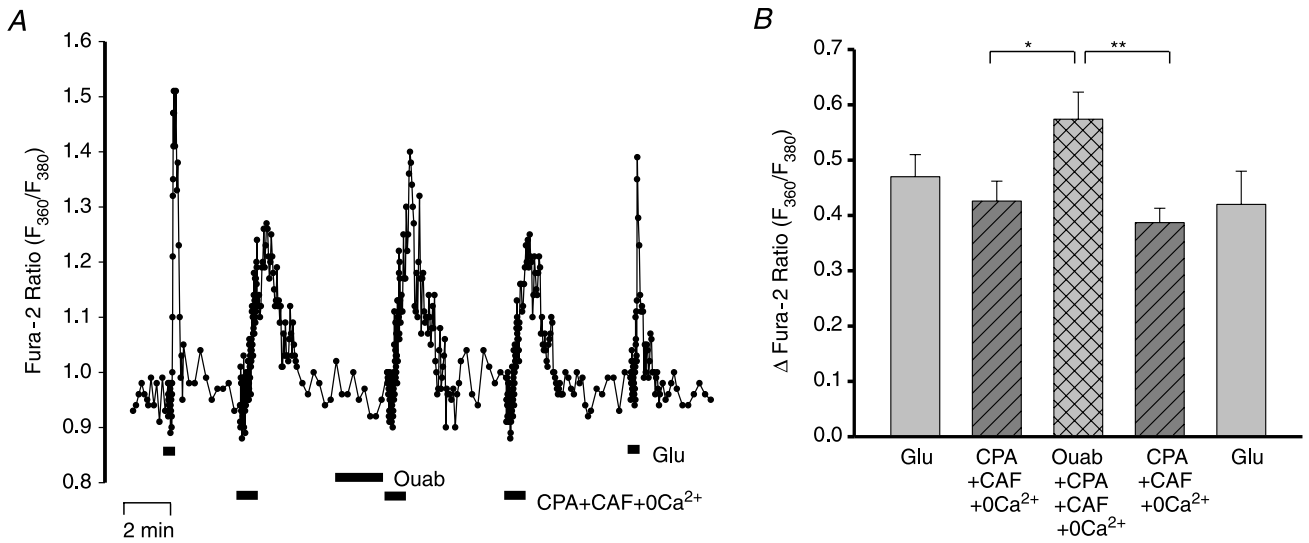

Figure 8. Effects of ouabain on releasable ER Ca^{2+} stores in neurones
A, F_{360}/F_{380} ratio data from a representative neurone in which the Ca^{2+} transients were evoked by 10 μM cyclopiazonic acid (CPA) + 10 mM caffeine (CAF) in Ca^{2+}-free medium. The response to CPA + CAF was tested before ouabain, immediately after a 4 min pretreatment with 3 nM ouabain, and following washout of the ouabain and recovery. *B*, averaged maximal increase (+SEM) in $\Delta F_{360}/F_{380}$ from experiments performed with the protocol shown in *A*. $n = 28$ cells; *$P < 0.05$, **$P < 0.01$ *vs.* before ouabain and after recovery, respectively (ANOVA).

Glu-evoked Ca^{2+} signals in the neurones are mediated by NCX.

Effects of nanomolar ouabain on Ca^{2+} signalling in astrocytes

The Ca^{2+} signalling in astrocytes, too, was augmented by pre-incubation with CTS. For example, in the experiment illustrated in Fig. 10*A*, 3 μM Glu evoked Ca^{2+} signals only in neurones (Fig. 10*Ab*, cells N1 and N2). After a 5 min pre-incubation with 3 nM ouabain, the neuronal response to 3 μM Glu was amplified (Fig. 10*Ac* and *B*), but the astrocytes then also exhibited small, delayed Ca^{2+} transients in response to the Glu (Fig. 10*Ab*, cells A1 and A2; Fig. 10*B*). The astrocytes were then identified by their responses to 0.5 μM ATP (Fig. 10*Ae*, cells A1 and A2; Fig. 10*B*), to which the neurons did not respond. The ATP-evoked Ca^{2+} signal in one astrocyte (A1) was amplified following a 5 min pre-incubation with 3 nM ouabain, but neither the other astrocyte nor the two neurones responded (Fig. 10*Ae* and *f* and *B*). Thus, 3 nM ouabain augments astrocyte responses to both ATP and Glu. Summary data for the effect of 3 nM ouabain on the 0.5 μM ATP-evoked Ca^{2+} signals in astrocytes are shown in

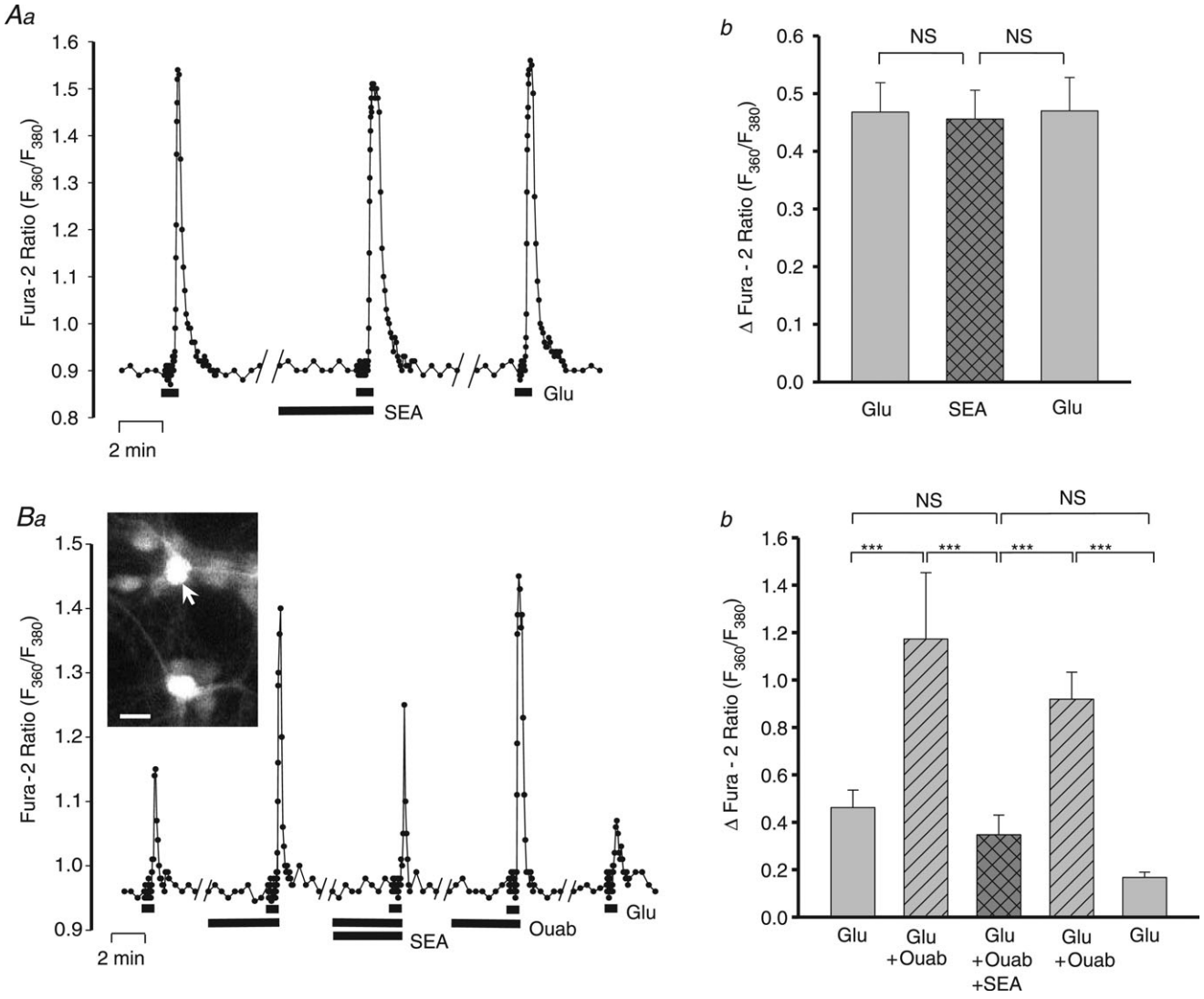

Figure 9. Effects of SEA0400 on the augmentation of Glu-evoked neuronal Ca^{2+} signals by ouabain
A, effects of 300 μM SEA0400 on the Ca^{2+} transients evoked by 3 μM Glu. SEA0400 was dissolved in DMSO (final concentration of 0.367%) which, alone, had no effect on the Ca^{2+} transients (data not shown, but see Fig. 3*B*). *Aa*, data from a representative neurone illustrate the protocol. *Ab*, summarized data from 11 neurones show that SEA0400 did not significantly affect the Glu-evoked Ca^{2+} signals. *B*, effect of 3 nM ouabain ± 300 μM SEA0400 on 3 μM Glu-evoked Ca^{2+} transients. *Ba*, data from a representative neurone; inset shows the neurone (arrow) sitting on a layer of astrocytes. *Bb*, summary of data from 11 neurones. NS, not significantly different; ***$P < 0.001$, for the indicated pairs (ANOVA).

Fig. 10*C*. These enhanced signals, too, are apparently the result of increased release of Ca^{2+} from the ER stores, because ouabain also augmented CPA + CAF-induced Ca^{2+} signals in astrocytes in Ca^{2+}-free conditions (Fig. 11).

Discussion

Rat hippocampal neurones express Na^+ pumps with an α3 catalytic subunit

We examined the roles of high-ouabain-affinity α2 and α3 Na^+ pumps in neurones and astrocytes co-cultured from rat hippocampus. Astrocytes express α2 Na^+ pumps (Fig. 1), in addition to α1 Na^+ pumps (McGrail *et al.* 1991; Brines & Robbins, 1993; Song *et al.* 2006). Our immunocytochemical data (Fig. 1) indicate, however, that all hippocampal neurones express both α3 and α1 Na^+ pumps, but not α2 Na^+ pumps (Juhaszova & Blaustein, 1997*a*,*b*).

The α2 and α3 subunits have 89% amino acid sequence identity, including the highly conserved high-ouabain-affinity binding site (Price *et al.* 1990), and the two isoforms have very similar ouabain affinities, with EC_{50} values of the order of 1 nM or less (Fig. 4*B*; Zhang, 2006; Raina *et al.* 2010). They also are both localized to PM microdomains at PM–ER junctions (Juhaszova & Blaustein, 1997*a*,*b*; Lencesova *et al.* 2004) and both thus help to regulate ER Ca^{2+} storage and Ca^{2+} signalling (see below Section on: Nanomolar concentrations of CTS increase ER Ca^{2+} stores and enhance mGluR-mediated Ca^{2+} signalling in neurones). The two isoforms have different affinities for intracellular Na^+; however, apparent K_m values for α2 and α3 are, respectively, 22 and 33 mM, *vs.* 12 mM for α1 (Zahler *et al.* 1997). This difference accounts for the fact that low concentrations of ouabain, acting only on α2 and α3 pumps, did not alter resting cytosolic $[Ca^{2+}]$ (e.g. Fig. 5*Aa*), which is regulated primarily by the more prevalent α1 pumps. Also, the α2 and α3 pumps might be regulated differently, e.g. in skeletal muscle, insulin

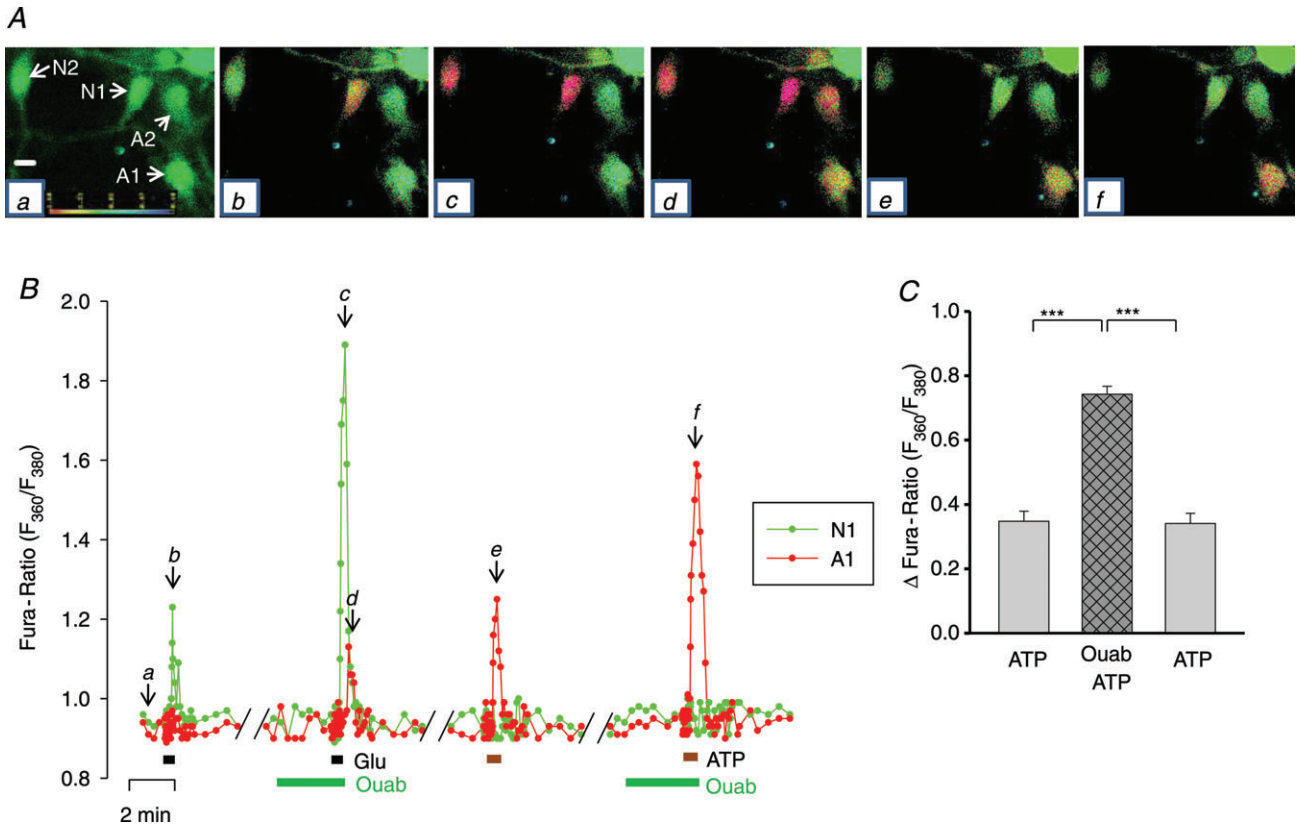

Figure 10. Effect of ouabain on Glu- and ATP-evoked Ca^{2+} transients in neurones and astrocytes
A, time course of the changes in the F_{360}/F_{380} ratio evoked by 3 μM Glu and 0.5 μM ATP in the absence and presence of 3 nM ouabain in two neurones (N1 and N2) and two astrocytes (A1 and A2). The F_{360}/F_{380} ratio pseudocolour images (*Aa*–*f*), captured at the time points indicated on the graph (*B*), show the ratio in, respectively, resting (basal) conditions (*Aa*) and at the peaks of the responses to Glu (*Ab*), Glu + ouabain (*Ac* and *d*), ATP (*Ae*) and ATP + ouabain (*Af*). The scale bar in *Aa* represents 20 μm. *B*, time course graph of the F_{360}/F_{380} ratio changes for cells A1 (red) and N1 (green). *C*, summary data from 13 astrocytes that were treated in a similar manner. Ouabain (3 nM) significantly increased the amplitude of the Ca^{2+} transients evoked by ATP (0.5 μM); ***$P < 0.001$ *vs.* ATP alone (ANOVA).

regulates $\alpha 2$ insertion into the PM (Hundal *et al.* 1992), but there is no information on comparable $\alpha 2$ or $\alpha 3$ Na^+ pump regulation in the brain.

Hippocampal neurones and astrocytes respond differently to glutamate, carbachol and ATP

Astrocytes and many neurones are activated by some of the same neurotransmitters (van den Pol *et al.* 1992; Araque *et al.* 2001; Halassa & Haydon, 2010). Here, we studied Ca^{2+} signalling evoked by Glu, 5-HT, CCh and ATP in neurones and astrocytes in rat hippocampal co-cultures. The neurones and astrocytes were distinguished by a combination of immunocytochemistry (Figs 1 and 2) and differences in their responses to the neurotransmitters.

Both neurones and astrocytes were activated by both Glu and ATP, but the transmitter concentration dependence and the Ca^{2+} signals differed in the two cell types. Neurones responded robustly to low-dose (3–4 μM) Glu, whereas the astrocytes either failed to respond or exhibited only small, delayed Ca^{2+} transients. Most astrocytes did, however, respond strongly to 5–10 μM Glu. In contrast, the neurones did not respond to low-dose (0.5–1 μM) ATP, whereas virtually all astrocytes gave robust responses. Much higher ATP concentrations (5–10 μM), however, evoked large Ca^{2+} transients in most neurones. Neurones, but not astrocytes, responded to bath-applied 3–10 μM CCh, and neither cell type responded to 5-HT. The implication is that the cultured neurones express muscarinic (metabotropic) acetylcholine receptors in addition to mGluRs, but do not express 5-HT receptors coupled to ER Ca^{2+} stores.

Importantly, the Glu-evoked Ca^{2+} signals in the neurones were unaffected by the NMDAR antagonist, AP5, or by low-dose LY341495, which is specific for type II mGluRs. The Ca^{2+} transients were markedly reduced by high-dose LY341495, which blocks most mGluRs (Kingston *et al.* 1998), and by the selective mGluR5 antagonist MPEP, but not by the mGluR1 antagonist, LY367385. Thus, we conclude that these responses to bath-applied Glu were mediated primarily by mGluR5, with subsequent generation of inositol trisphosphate and release of Ca^{2+} from ER stores (Nakamura *et al.* 2000), and not by NMDAR-mediated influx of Ca^{2+} from the extracellular fluid. This does not mean that NMDARs in the neurones were not activated by the Glu, because small, brief Ca^{2+} transients activated by rapidly opening and closing NMDAR channels would have been missed by the relatively slow rate of image capture (3 ratio images s^{-1}). Nevertheless, these methods were well suited for studying the slower events described in the next section.

Nanomolar concentrations of CTS increase ER Ca^{2+} stores and enhance mGluR-mediated Ca^{2+} signalling in neurones

Acutely administered ouabain, at concentrations of 1–10 nM, greatly increased the neuronal Ca^{2+} transients

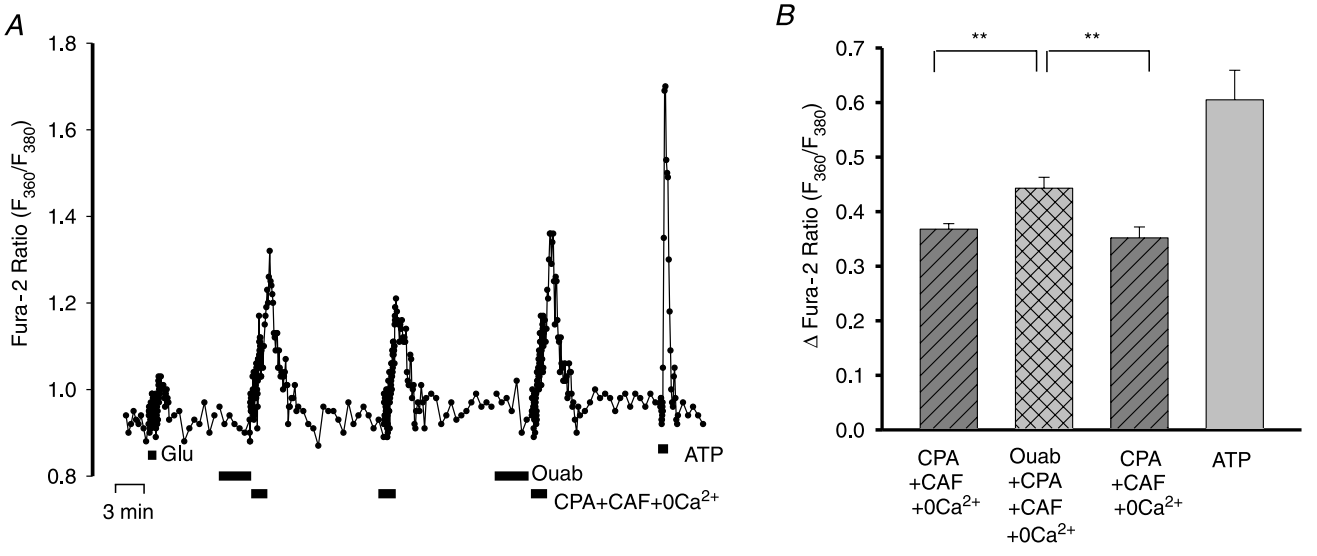

Figure 11. Effects of ouabain on releasable endoplasmic reticulum Ca^{2+} stores in astrocytes
A, F_{360}/F_{380} ratio data from a representative astrocyte in which the Ca^{2+} transients were evoked by 10 μM CPA + 10 mM CAF in Ca^{2+}-free medium; the cell responded robustly to 0.5 μM ATP but only slightly to 4 μM Glu. The response to CPA + CAF was tested before ouabain and immediately after a 4 min pretreatment with 3 nM ouabain. *B*, averaged maximal increase (+SEM) in $\Delta F_{360}/F_{380}$ in response to ATP and to CPA+CAF before and immediately after 3 nM ouabain, from experiments similar to the one shown in *A*. $n = 14$ cells; $^{**}P < 0.01$ *vs.* 'before' and 'after' ouabain (ANOVA).

evoked by 3–4 μM Glu. In a more limited set of experiments, 3–10 nM digoxin, the clinically used CTS, another Na^+ pump inhibitor, also augmented the Ca^{2+} transients (Fig. 5). Likewise, 3 nM ouabain enhanced the CCh-evoked Ca^{2+} transients (Fig. 7). The ouabain concentrations used in these studies are about an order of magnitude higher than the levels of endogenous ouabain in normal humans and rodents (0.15–0.6 nM; Manunta *et al.* 2006; Jacobs *et al.* 2012). Relatively high concentrations were used here to obtain large, readily measureable effects. The extrapolated data (Fig. 5*B*) indicate, however, that smaller but similar effects can be expected in the physiological range of endogenous ouabain (EO) concentrations as well as clinically relevant digoxin concentrations. The effects of nanomolar ouabain were mediated by α3 (and, in astrocytes, α2) Na^+ pumps, because the ouabain EC_{50} for α1 Na^+ pumps is ~5–10 μM in rodents (Zhang *et al.* 2005) and ~10–50 nM in humans (Linde *et al.* 2012), *vs.* ≈0.5 nM for α3 (Fig. 5*B*) and α2 (Zhang *et al.* 2005; Raina *et al.* 2010).

The mechanism of enhanced Ca^{2+} signalling involves CTS inhibition of the α3 Na^+ pumps, and local gain of Ca^{2+}, mediated by NCX, at the PM–ER junctions. The Ca^{2+} is then rapidly sequestered in the ER, because we did not detect a significant increase in the basal cytosolic Ca^{2+} concentration (i.e. in the fura-2 F_{360}/F_{380} ratio before or after the Ca^{2+} transient). The role of NCX was verified by blocking the Ca^{2+} signal augmentation with SEA0400 (Fig. 9), and the increase in ER $[Ca^{2+}]$ was detected as an increase in the CPA + CAF-releasable ER Ca^{2+} store (Fig. 8). The increase in ER $[Ca^{2+}]$ readily explains the enhanced Ca^{2+} release from the ER by an inositol trisphosphate-dependent mechanism (Nakamura *et al.* 2000). The proteins involved in this mechanism are not confined to the soma, but are also found in the axons and dendrites (e.g. Fig. 1*D* shows the distribution of α3 Na^+ pumps); thus, it is not surprising that ouabain-dependent Ca^{2+} signal augmentation is observed in neuronal axons and dendrites, as well as the soma (Fig. 6).

In the experiments illustrated in Fig. 8, external Ca^{2+} was restored when the Ca^{2+} transients peaked (see Fig. 8*A*) to avoid the deleterious effects of prolonged exposure to Ca^{2+}-free media. Thus, we cannot rule out a contribution to the transient from Ca^{2+} entry through store-operated cation channels as a result of the ER store depletion (Koss *et al.* 2009). These channels can admit both Ca^{2+} and Na^+ (Venkatachalam & Montell, 2007; Bollimuntha *et al.* 2011; Nilius & Owsianik, 2011). Activation of mGluRs also depolarizes hippocampal neurones (Crepel *et al.* 1994), which should promote Ca^{2+} gain through the voltage-sensitive NCX (Blaustein & Lederer, 1999). Importantly, the ouabain-induced inhibition of Na^+ extrusion and the entry of Na^+ through store-operated cation channels will raise the local intracellular Na^+ concentration ($[Na^+]_i$) at PM–ER junctions (Arnon *et al.* 2000). This should contribute to net Ca^{2+} gain via the adjacent NCX (Blaustein *et al.* 2002).

Ouabain also augments Ca^{2+} signalling in astrocytes

Nanomolar ouabain also amplifies the Ca^{2+} signals in astrocytes. For example, 3 nM ouabain often enabled low-dose (3–4 μM) Glu to evoke a Ca^{2+} transient in astrocytes when none was observed with Glu alone (Fig. 10*Ab* and *d*). The Ca^{2+} transients evoked by a low (0.5 μM) ATP concentration were virtually always augmented by 3 nM ouabain (Fig. 10*Ae* and *f*, *B* and *C*). Moreover, the mechanisms responsible for the effect of ouabain in astrocytes appear to be NCX- and ER Ca^{2+} store-dependent as in the neurones; in astrocytes, however, they involve Na^+ pumps with an α2 subunit.

In sum, these results indicate that the amplifying effects of acutely administered, low-dose CTS on Ca^{2+} signalling are quite broad. They are observed in both neurones and astrocytes, which have different high-ouabain-affinity receptor/Na^+ pumps, α3 and α2, respectively, and even in different types of neurones, such as bipolar cells and pyramidal cells (Fig. 5*A*). They are observed when several different types of receptors are activated, and are therefore not limited to any specific transmitter receptor. They also are not limited to a single type of CTS, because ouabain is a hydrophilic *Strophanthus* steroid and digoxin is a hydrophobic *Digitalis* steroid.

Physiological and pathophysiological implications

The findings reported here suggest that modest changes in the activity of Na^+ pumps with an α3 or α2 subunit may profoundly influence Ca^{2+} signalling and, thus, modulate neuronal and glial function in the brain. While the specific neuronal pathways have not been elucidated, it is reasonable to speculate that the manifestations of rapid-onset dystonia with parkinsonism are attributable to altered neuronal Ca^{2+} signals as a result of the loss-of-function mutations in the α3 subunit (equivalent to a low dose of ouabain). Altered Ca^{2+} signalling may also account for the manifestations of familial hemiplegic migraine. The three types of familial hemiplegic migraine are linked to, respectively, gain-of-function mutations in neuronal Ca^{2+} ($Ca_V1.2$) channels and Na^+ ($Na_V1.2$) channels and loss-of-function mutations in the Na^+ pump α2 subunit (Iribe *et al.* 2009; Morth *et al.* 2009; Bottger *et al.* 2012). The Na^+ pump and Na^+ channel defects may be expected to alter Ca^{2+} homeostasis indirectly, by raising $[Na^+]_i$ and thereby promoting Ca^{2+} entry through NCX. Here, too, the specific cells/pathways that give rise to the hemiplegia and the migraine are not known; neurons, astrocytes and even arterial myocytes, which also express α2 Na^+ pumps (Zhang, 2006), may be involved. In this

regard, it is noteworthy that astrocytes can modulate synaptic transmission at central synapses (Panatier *et al.* 2011) and that Na^+ pumps can mediate Glu-induced long-term effects on neuronal excitability and synaptic transmission (Nathanson *et al.* 1995).

The implications of our results for behavioural disorders are also worth consideration. As noted in the Introduction, a number of reports have linked bipolar mood disorders to reduced $\alpha2$ or $\alpha3$ Na^+ pump activity or to an endogenous ouabain-like compound (Goldstein *et al.* 2006, 2011). Indeed, endogenous ouabain may be synthesized and secreted in the brain (hypothalamus) as well as in the adrenal cortex (Laredo *et al.* 1994; Kawamura *et al.* 1999; Blaustein *et al.* 2012). Well-controlled follow-up studies may provide new insight into the neuronal pathways involved in mood regulation. Moreover, detailed neurophysiological study of the specific neuronal pathways that are affected by both the Na^+ pump mutations and the intracerebroventricular infusion of ouabain may provide insight into why some pathways seem to be more vulnerable than others to these global changes in $\alpha2$ and/or $\alpha3$ function.

References

Anderson TR, Huguenard JR & Prince DA (2010). Differential effects of Na^+–K^+ ATPase blockade on cortical layer V neurons. *J Physiol* **588**, 4401–4414.

Annunziato L, Pignataro G & Di Renzo GF (2004). Pharmacology of brain Na^+/Ca^{2+} exchanger: from molecular biology to therapeutic perspectives. *Pharmacol Rev* **56**, 633–654.

Araque A, Carmignoto G & Haydon PG (2001). Dynamic signaling between astrocytes and neurons. *Ann Rev Physiol* **63**, 795–813.

Arnon A, Hamlyn JM & Blaustein MP (2000). Ouabain augments Ca^{2+} transients in arterial smooth muscle without raising cytosolic Na^+. *Am J Physiol Heart Circ Physiol* **279**, H679–H691.

Blanco G & Mercer RW (1998). Isozymes of the Na-K-ATPase: heterogeneity in structure, diversity in function. *Am J Physiol Renal Physiol* **275**, F633–F650.

Blaustein MP (1993). Physiological effects of endogenous ouabain: control of intracellular Ca^{2+} stores and responsiveness. *Am J Physiol Cell Physiol* **264**, C1367–C1387.

Blaustein MP & Golovina VA (2001). Structural complexity and functional diversity of endoplasmic reticulum Ca^{2+} stores. *Trends Neurosci* **24**, 602–608.

Blaustein MP, Juhaszova M, Golovina VA, Church PJ & Stanley EF (2002). Na/Ca exchanger and PMCA localization in neurons and astrocytes: functional implications. *Ann N Y Acad Sci* **976**, 356–366.

Blaustein MP & Lederer WJ (1999). Sodium/calcium exchange: its physiological implications. *Physiol Rev* **79**, 763–854.

Blaustein MP, Leenen FH, Chen L, Golovina VA, Hamlyn JM, Pallone TL, Van Huysse JW, Zhang J & Wier WG (2012). How NaCl raises blood pressure: a new paradigm for the pathogenesis of salt-dependent hypertension. *Am J Physiol Heart Circ Physiol* **302**, H1031–H1049.

Blaustein MP & Wiesmann WP (1970). Effect of sodium ions on calcium movements in isolated synaptic terminals. *Proc Natl Acad Sci U S A* **66**, 664–671.

Bollimuntha S, Selvaraj S & Singh BB (2011). Emerging roles of canonical TRP channels in neuronal function. *Adv Exp Med Biol* **704**, 573–593.

Bottger P, Doganli C & Lykke-Hartmann K (2012). Migraine- and dystonia-related disease-mutations of Na^+/K^+-ATPases: relevance of behavioral studies in mice to disease symptoms and neurological manifestations in humans. *Neurosci Biobehav Rev* **36**, 855–871.

Brashear A, Dobyns WB, de Carvalho Aguiar P, Borg M, Frijns CJ, Gollamudi S, Green A, Guimaraes J, Haake BC, Klein C, Linazasoro G, Münchau A, Raymond D, Riley D, Saunders-Pullman R, Tijssen MA, Webb D, Zaremba J, Bressman SB & Ozelius LJ (2007). The phenotypic spectrum of rapid-onset dystonia–parkinsonism (RDP) and mutations in the *ATP1A3* gene. *Brain* **130**, 828–835.

Brines ML & Robbins RJ (1993). Cell-type specific expression of Na^+,K^+-ATPase catalytic subunits in cultured neurons and glia: evidence for polarized distribution in neurons. *Brain Res* **631**, 1–11.

Coppen A, Shaw DM, Malleson A & Costain R (1966). Mineral metabolism in mania. *Br Med J* **1**, 71–75.

Crepel V, Aniksztejn L, Ben-Ari Y & Hammond C (1994). Glutamate metabotropic receptors increase a Ca^{2+}-activated nonspecific cationic current in CA1 hippocampal neurons. *J Neurophysiol* **72**, 1561–1569.

de Carvalho Aguiar P, Sweadner KJ, Penniston JT, Zaremba J, Liu L, Caton M, Linazasoro G, Borg M, Tijssen MA, Bressman SB, Dobyns WB, Brashear A & Ozelius LJ (2004). Mutations in the Na^+/K^+-ATPase $\alpha3$ gene *ATP1A3* are associated with rapid-onset dystonia parkinsonism. *Neuron* **43**, 169–175.

De Fusco M, Marconi R, Silvestri L, Atorino L, Rampoldi L, Morgante L, Ballabio A, Aridon P & Casari G (2003). Haploinsufficiency of *ATP1A2* encoding the Na^+/K^+ pump $\alpha2$ subunit associated with familial hemiplegic migraine type 2. *Nat Genet* **33**, 192–196.

de Vries B, Freilinger T, Vanmolkot KR, Koenderink JB, Stam AH, Terwindt GM, Babini E, van den Boogerd EH, van den Heuvel JJ, Frants RR, Haan J, Pusch M, van den Maagdenberg AM, Ferrari MD & Dichgans M (2007). Systematic analysis of three FHM genes in 39 sporadic patients with hemiplegic migraine. *Neurology* **69**, 2170–2176.

Dostanic I, Paul RJ, Lorenz JN, Theriault S, Van Huysse JW & Lingrel JB (2005). The α_2-isoform of Na-K-ATPase mediates ouabain-induced hypertension in mice and increased vascular contractility in vitro. *Am J Physiol Heart Circ Physiol* **288**, H477–H485.

Dostanic-Larson I, Van Huysse JW, Lorenz JN & Lingrel JB (2005). The highly conserved cardiac glycoside binding site of Na,K-ATPase plays a role in blood pressure regulation. *Proc Natl Acad Sci U S A* **102**, 15845–15850.

El-Mallakh RS, Decker S, Morris M, Li XP, Huff MO, El-Masri MA & Levy RS (2006). Efficacy of olanzapine and haloperidol in an animal model of mania. *Prog Neuropsychopharmacol Biol Psychiatry* **30**, 1261–1264.

El-Mallakh RS, El-Masri MA, Huff MO, Li XP, Decker S & Levy RS (2003). Intracerebroventricular administration of ouabain as a model of mania in rats. *Bipolar Disord* **5**, 362–365.

Goldstein I, Lax E, Gispan-Herman I, Ovadia H, Rosen H, Yadid G & Lichtstein D (2011). Neutralization of endogenous digitalis-like compounds alters catecholamines metabolism in the brain and elicits anti-depressive behavior. *Eur Neuropsychopharmacol* **22**, 72–79.

Goldstein I, Levy T, Galili D, Ovadia H, Yirmiya R, Rosen H & Lichtstein D (2006). Involvement of Na^+, K^+-ATPase and endogenous digitalis-like compounds in depressive disorders. *Biol Psychiatry* **60**, 491–499.

Golovina VA, Song H, James PF, Lingrel JB & Blaustein MP (2003). Na^+ pump α_2-subunit expression modulates Ca^{2+} signaling. *Am J Physiol Cell Physiol* **284**, C475–C486.

Halassa MM & Haydon PG (2010). Integrated brain circuits: astrocytic networks modulate neuronal activity and behavior. *Ann Rev Physiol* **72**, 335–355.

Hamid H, Gao Y, Lei Z, Hougland MT & El-Mallakh RS (2009). Effect of ouabain on sodium pump alpha-isoform expression in an animal model of mania. *Prog Neuropsychopharmacol Biol Psychiatry* **33**, 1103–1106.

Hamlyn JM, Blaustein MP, Bova S, DuCharme DW, Harris DW, Mandel F, Mathews WR & Ludens JH (1991). Identification and characterization of a ouabain-like compound from human plasma. *Proc Natl Acad Sci U S A* **88**, 6259–6263.

Hundal HS, Marette A, Mitsumoto Y, Ramlal T, Blostein R & Klip A (1992). Insulin induces translocation of the α2 and β1 subunits of the Na^+/K^+-ATPase from intracellular compartments to the plasma membrane in mammalian skeletal muscle. *J Biol Chem* **267**, 5040–5043.

Ikeda K, Onaka T, Yamakado M, Nakai J, Ishikawa TO, Taketo MM & Kawakami K (2003). Degeneration of the amygdala/piriform cortex and enhanced fear/anxiety behaviors in sodium pump α2 subunit (*Atp1a2*)-deficient mice. *J Neurosci* **23**, 4667–4676.

Iribe G, Ward CW, Camelliti P, Bollensdorff C, Mason F, Burton RA, Garny A, Morphew MK, Hoenger A, Lederer WJ & Kohl P (2009). Axial stretch of rat single ventricular cardiomyocytes causes an acute and transient increase in Ca^{2+} spark rate. *Circ Res* **104**, 787–795.

Iwamoto T, Watanabe Y, Kita S & Blaustein MP (2007). Na^+/Ca^{2+} exchange inhibitors: a new class of calcium regulators. *Cardiovasc Hematol Disord Drug Targets* **7**, 188–198.

Jacobs BE, Liu Y, Pulina MV, Golovina VA & Hamlyn JM (2012). Normal pregnancy: mechanisms underlying the paradox of a ouabain-resistant state with elevated endogenous ouabain, suppressed arterial sodium calcium exchange, and low blood pressure. *Am J Physiol Heart Circ Physiol* **302**, H1317–H1329.

Juhaszova M & Blaustein MP (1997*a*). Distinct distribution of different Na^+ pump α subunit isoforms in plasmalemma. Physiological implications. *Ann N Y Acad Sci* **834**, 524–536.

Juhaszova M & Blaustein MP (1997*b*). Na^+ pump low and high ouabain affinity α subunit isoforms are differently distributed in cells. *Proc Natl Acad Sci U S A* **94**, 1800–1805.

Kawamura A, Guo J, Itagaki Y, Bell C, Wang Y, Haupert GT Jr, Magil S, Gallagher RT, Berova N & Nakanishi K (1999). On the structure of endogenous ouabain. *Proc Natl Acad Sci U S A* **96**, 6654–6659.

Kingston AE, Ornstein PL, Wright RA, Johnson BG, Mayne NG, Burnett JP, Belagaje R, Wu S & Schoepp DD (1998). LY341495 is a nanomolar potent and selective antagonist of group II metabotropic glutamate receptors. *Neuropharmacology* **37**, 1–12.

Kirshenbaum GS, Clapcote SJ, Duffy S, Burgess CR, Petersen J, Jarowek KJ, Yucel YH, Cortez MA, Snead OC 3rd, Vilsen B, Peever JH, Ralph MR & Roder JC (2011). Mania-like behavior induced by genetic dysfunction of the neuron-specific Na^+,K^+-ATPase α3 sodium pump. *Proc Natl Acad Sci U S A* **108**, 18144–18149.

Koss DJ, Riedel G & Platt B (2009). Intracellular Ca^{2+} stores modulate SOCCs and NMDA receptors via tyrosine kinases in rat hippocampal neurons. *Cell Calcium* **46**, 39–48.

Laredo J, Hamilton BP & Hamlyn JM (1994). Ouabain is secreted by bovine adrenocortical cells. *Endocrinology* **135**, 794–797.

Lee MY, Song H, Nakai J, Ohkura M, Kotlikoff MI, Kinsey SP, Golovina VA & Blaustein MP (2006). Local subplasma membrane Ca^{2+} signals detected by a tethered Ca^{2+} sensor. *Proc Natl Acad Sci U S A* **103**, 13232–13237.

Lencesova L, O'Neill A, Resneck WG, Bloch RJ & Blaustein MP (2004). Plasma membrane-cytoskeleton-endoplasmic reticulum complexes in neurons and astrocytes. *J Biol Chem* **279**, 2885–2893.

Linde CI, Antos LK, Golovina VA & Blaustein MP (2012). Nanomolar ouabain increases NCX1 expression and enhances Ca^{2+} signaling in human arterial myocytes: a mechanism that links salt to increased vascular resistance? *Am J Physiol Heart Circ Physiol* **303**, H784–H794.

Lingrel JB (2010). The physiological significance of the cardiotonic steroid/ouabain-binding site of the Na,K-ATPase. *Ann Rev Physiol* **72**, 395–412.

Lingrel JB, Williams MT, Vorhees CV & Moseley AE (2007). Na,K-ATPase and the role of α isoforms in behavior. *J Bioenerg Biomembr* **39**, 385–389.

Looney SW & el-Mallakh RS (1997). Meta-analysis of erythrocyte Na,K-ATPase activity in bipolar illness. *Depress Anxiety* **5**, 53–65.

McGrail KM, Phillips JM & Sweadner KJ (1991). Immunofluorescent localization of three Na,K-ATPase isozymes in the rat central nervous system: both neurons and glia can express more than one Na,K-ATPase. *J Neurosci* **11**, 381–391.

Mannaioni G, Marino MJ, Valenti O, Traynelis SF & Conn PJ (2001). Metabotropic glutamate receptors 1 and 5 differentially regulate CA1 pyramidal cell function. *J Neurosci* **21**, 5925–5934.

Manunta P, Hamilton BP & Hamlyn JM (2006). Salt intake and depletion increase circulating levels of endogenous ouabain in normal men. *Am J Physiol Regul Integr Comp Physiol* **290**, R553–R559.

Morth JP, Poulsen H, Toustrup-Jensen MS, Schack VR, Egebjerg J, Andersen JP, Vilsen B & Nissen P (2009). The structure of the Na^+,K^+-ATPase and mapping of isoform differences and disease-related mutations. *Philos Trans R Soc Lond B Biol Sci* **364**, 217–227.

Moseley AE, Lieske SP, Wetzel RK, James PF, He S, Shelly DA, Paul RJ, Boivin GP, Witte DP, Ramirez JM, Sweadner KJ & Lingrel JB (2003). The Na,K-ATPase α2 isoform is expressed in neurons, and its absence disrupts neuronal activity in newborn mice. *J Biol Chem* **278**, 5317–5324.

Moseley AE, Williams MT, Schaefer TL, Bohanan CS, Neumann JC, Behbehani MM, Vorhees CV & Lingrel JB (2007). Deficiency in Na,K-ATPase α isoform genes alters spatial learning, motor activity, and anxiety in mice. *J Neurosci* **27**, 616–626.

Nakamura T, Nakamura K, Lasser-Ross N, Barbara JG, Sandler VM & Ross WN (2000). Inositol 1,4,5-trisphosphate (IP_3)-mediated Ca^{2+} release evoked by metabotropic agonists and backpropagating action potentials in hippocampal CA1 pyramidal neurons. *J Neurosci* **20**, 8365–8376.

Nathanson JA, Scavone C, Scanlon C & McKee M (1995). The cellular Na^+ pump as a site of action for carbon monoxide and glutamate: a mechanism for long-term modulation of cellular activity. *Neuron* **14**, 781–794.

Naylor GJ, McNamee HB & Moody JP (1970). Erythrocyte sodium and potassium in depressive illness. *J Psychosom Res* **14**, 173–177.

Naylor GJ & Smith AH (1981). Defective genetic control of sodium-pump density in manic depressive psychosis. *Psychol Med* **11**, 257–263.

Nilius B & Owsianik G (2011). The transient receptor potential family of ion channels. *Genome Biol* **12**, 218.

O'Brien WJ, Lingrel JB & Wallick ET (1994). Ouabain binding kinetics of the rat alpha two and alpha three isoforms of the sodium-potassium adenosine triphosphate. *Arch Biochem Biophys* **310**, 32–39.

Panatier A, Vallee J, Haber M, Murai KK, Lacaille JC & Robitaille R (2011). Astrocytes are endogenous regulators of basal transmission at central synapses. *Cell* **146**, 785–798.

Pressley TA (1992). Phylogenetic conservation of isoform-specific regions within alpha-subunit of Na^+-K^+-ATPase. *Am J Physiol Cell Physiol* **262**, C743–C751.

Price EM, Rice DA & Lingrel JB (1990). Structure-function studies of Na,K-ATPase. Site-directed mutagenesis of the border residues from the H1-H2 extracellular domain of the α subunit. *J Biol Chem* **265**, 6638–6641.

Raina H, Zhang Q, Rhee AY, Pallone TL & Wier WG (2010). Sympathetic nerves and endothelium influence the vasoconstrictor effect of low concentrations of ouabain in pressurized small arteries. *Am J Physiol Heart Circ Physiol* **298**, H2093–H2101.

Reich CG, Mason SE & Alger BE (2004). Novel form of LTD induced by transient, partial inhibition of the Na,K-pump in rat hippocampal CA1 cells. *J Neurophysiol* **91**, 239–247.

Riaza Bermudo-Soriano C, Perez-Rodriguez MM, Vaquero-Lorenzo C & Baca-Garcia E (2012). New perspectives in glutamate and anxiety. *Pharmacol Biochem Behav* **100**, 752–774.

Richards KS, Bommert K, Szabo G & Miles R (2007). Differential expression of Na^+/K^+-ATPase α-subunits in mouse hippocampal interneurones and pyramidal cells. *J Physiol* **585**, 491–505.

Rose AM, Mellett BJ, Valdes R Jr, Kleinman JE, Herman MM, Li R & el-Mallakh RS (1998). Alpha2 isoform of the Na,K-adenosine triphosphatase is reduced in temporal cortex of bipolar individuals. *Biol Psychiatry* **44**, 892–897.

Schaefer TL, Lingrel JB, Moseley AE, Vorhees CV & Williams MT (2011). Targeted mutations in the Na,K-ATPase alpha 2 isoform confer ouabain resistance and result in abnormal behavior in mice. *Synapse* **65**, 520–531.

Schoner W & Scheiner-Bobis G (2007). Endogenous and exogenous cardiac glycosides: their roles in hypertension, salt metabolism, and cell growth. *Am J Physiol Cell Physiol* **293**, C509–C536.

Sohn JW, Lee D, Cho H, Lim W, Shin HS, Lee SH & Ho WK (2007). Receptor-specific inhibition of $GABA_B$-activated K^+ currents by muscarinic and metabotropic glutamate receptors in immature rat hippocampus. *J Physiol* **580**, 411–422.

Song H, Lee MY, Kinsey SP, Weber DJ & Blaustein MP (2006). An N-terminal sequence targets and tethers Na^+ pump α2 subunits to specialized plasma membrane microdomains. *J Biol Chem* **281**, 12929–12940.

Vaillend C, Mason SE, Cuttle MF & Alger BE (2002). Mechanisms of neuronal hyperexcitability caused by partial inhibition of Na^+-K^+-ATPases in the rat CA1 hippocampal region. *J Neurophysiol* **88**, 2963–2978.

van den Pol AN, Finkbeiner SM & Cornell-Bell AH (1992). Calcium excitability and oscillations in suprachiasmatic nucleus neurons and glia *in vitro*. *J Neuroscience* **12**, 2648–2664.

Venkatachalam K & Montell C (2007). TRP channels. *Ann Rev Biochem* **76**, 387–417.

Verderio C & Matteoli M (2011). ATP in neuron–glia bidirectional signalling. *Brain Res Rev* **66**, 106–114.

Yarowsky PJ & Krueger BK (1989). Development of saxitoxin-sensitive and insensitive sodium channels in cultured neonatal rat astrocytes. *J Neuroscience* **9**, 1055–1061.

Zahler R, Zhang ZT, Manor M & Boron WF (1997). Sodium kinetics of Na,K-ATPase α isoforms in intact transfected HeLa cells. *J Gen Physiol* **110**, 201–213.

Zhang J, Chen L, Lingrel JB, Philipson KD & Blaustein MP (2006). Arterial myocyte Na^+ pumps and Na^+/Ca^{2+} exchangers modulate Ca^{2+} signaling, contractility and long-term blood pressure. *J Hypertens* **24**(Suppl. 6), S61.

Zhang J, Lee MY, Cavalli M, Chen L, Berra-Romani R, Balke CW, Bianchi G, Ferrari P, Hamlyn JM, Iwamoto T, Lingrel JB, Matteson DR, Wier WG & Blaustein MP (2005). Sodium pump α2 subunits control myogenic tone and blood pressure in mice. *J Physiol* **569**, 243–256.

Zhang Z & Seguela P (2010). Metabotropic induction of persistent activity in layers II/III of anterior cingulate cortex. *Cereb Cortex* **20**, 2948–2957.

Zhu L, Strata P & Andjus PR (2005). Pharmacology of the metabotropic glutamate receptor mediated current at the climbing fiber to Purkinje cell synapse. *Prog Brain Res* **148**, 299–306.

Author contributions

M.P.B, H.S. and S.M.T. designed the experiments. H.S. performed the experiments. H.S. and M.P.B. analysed the data, and M.P.B., H.S. and S.M.T. interpreted the results. M.P.B. and H.S. drafted the manuscript. All three authors edited and approved the final manuscript.

Acknowledgements

We thank Dr B. E. Alger for help regarding the glutamate receptor blockers and the activation of acetylcholine receptors. This work was supported by NIH grants NS16106, HL45215 and HL107555.